EFFECT OF NOISE ON OPTICAL FREQUENCY COMB

A Dissertation

Submitted in Partial Fulfillment of the Requirement for the Award of Degree of

Master of Science

In

Physics

Submitted By:

Manpreet kaur

Roll No. 302004010

Under the supervision of:

Dr.SOUMENDU JANA

Professor

TIET Patiala

THAPAR INSTITUTE
OF ENGINEERING & TECHNOLOGY
(Deemed to be University)

SCHOOL OF PHYSICS AND MATERIALS SCIENCE

THAPAR INSTITUTE OF ENGINEERING AND TECHNOLOGY,PATIALA

PUNJAB-140701

I dedicated this work to my family

and friends who supported me.

Certificate

I hereby declare that the work presented in this thesis entitled"EFFECT OF NOISE ON OPTICAL FREQUENCY COMB" is an authentic record of my own work carried out for the partial fulfillment of the requirement for the award of the degree of Master of Science in Physics at Thapar Institute of Engineering and Technology, Patiala, Punjab, under the guidance of Dr. Soumendu Jana, Professor, School of Physics and Materials Science and refers to other researcher's work, duly listed in the reference section. The intellectual content of this thesis is the product of my own work and contains no material which to a substantial extent has been accepted for the award of any other degree at this or any other educational institution, except where due acknowledgement is made in the thesis.

Dated: 25-7-2022

Manpreet Kaur

(Manpreet Kaur)

302004010

It is to certify that the above statement made by the candidate is correct and true to the best of my knowledge and belief.

Soumendu Jana

(Dr. Soumendu Jana)

Professor

School of Physics and Materials Science

TIET, Patiala

Acknowledgment

Work on this thesis would not have been possible without the encouragement and support of many people. It is a pleasure to convey my sincere gratitude and appreciation to all of them in my humble acknowledgement. First and greatest thank to my supervisor Dr. Soumendu Jana for his continuous supervision, guidance, patience, motivation and emotional support. Without his knowledge and support this work would not have been successful. I sincerely thank him from the bottom of my heart. I wish to express my sincere thanks to Dr. Kulvir Singh, Professor and Head, School of Physics and Materials Science, Thapar Institute of Engineering and Technology, Patiala for providing me all the necessary facilities for my research. Besides, my supervisor, I express my heartfelt gratitude to Mr. Neeraj Sharma, Ms.Jaspreet Kaur, Mr. Vikas, Ms.Anjali Saini, and Ms.Gurpreet kaur Research Scholars have always been there for me with their supporting hands whenever I needed them. Also thanks for sharing their valuable experiences with me. I would not have been able to complete my thesis without their cooperation. Last but not least, I acknowledge the people who mean a lot to me, my parents, younger sister and brother, whose selfless love, support and care gave me the strength to complete my dissertation. Also, I would like to thank them for their unconditional financial and emotional support throughout my degree. Above all I render my gratitude to the almighty who bestowed upon me the strength and vision to walk on the path of truth.

(Manpreet kaur)

Contents

List of Figures

Abstract

In this thesis work, we study the effect of noise on the optical frequency comb. We consider a microresonator system made of a vertical surface-emitting laser with a graphene saturable absorber. The investigation is done by solving the complex Ginzburg-Landau equation that represents the microresonator system. The split-step Fourier method-based code is used to solve the governing equation and to get the optical frequency comb. The different range of optical frequency comb is identified. Different sets of optical frequency comb are observed for the different ranges of the signal-to-noise ratio. We study how the optical frequency comb changes with a change in the operating wavelength. These results may help in the enhancement of the performance of optical frequency comb.

Chapter 1

Introduction

1.1 Introduction to optical frequency comb

In modern times the physical quantity which can be find out with very high precision and accuracy and stability is frequency. Optical frequency comb (OFC) is a device used to measure frequencies precisely. It is a ruler like tool for light frequencies [1]. It has a comb-like structure with in general, equally spaced lines(teeth). It was primarily developed to count the cycles from optical atomic clocks [2]. In other words OFC is an optical clockwork gear [4]. OFC is a synthesizer which can synthesize the frequency in the desired frequency comb domain [3]. If we zoom into the comb spectrum, there are multiple teeth. The space between the teeth depends on the time separation between the pulse train. The bandwidth of the OFC depends on the shortness of the pulse train. It can be associated with the regular train of ultrashort pulses [8], which has a fixed repetition rate. The properties of light in time domain are converted into frequency domain, which look like a comb. It permits a coherent connection between optical frequencies of the femtosecond time scale with the radio frequencies. The simple concept of OFC and their flexibility turned them into a powerful tool to measure high frequencies very accurately and opened many frontiers in various research fields where in scientists use to measure and control light waves [4,9].

OFC is a Nobel prize-winning device. Theodor W.Hansch and John L.Hall win a Noble prize in 2005 for developing a laser-based OFC [5]. John Hall's group at University of Colorado Boulder invented the comb. The National Institute of Standards and University of Colorado Boulder formed a joint institute where in the research on OFC was continued[6]. In 1993, after various experiments, research showed a new path of frequency measurements, which is the comb-like mode spectrum of a femtosecond laser [7]. Furthermore, it is demonstrated for the ultraviolet range. This enables frequency related measurment i.e., frequency metrology in the ultraviolet region.

Optical frequency comb has a wide area of applications such as precision ranging, molecular fingerprinting, coherent control, trace gas sensing in the oil industry [1], medical field,high precision spectroscopy, optical metrology, optical atomic clock, frequency chain generation, and more precise GPS technology [5]. In fact, this is increasing day by day.

There are various methods to generate a frequency comb. These are demonstrated by different mechanisms such as a mode-locked laser, four waves mixing in a non-linear medium, periodic modulation of a continuous-wave laser, and stabilization of the pulse train [5]. The ways to generate OFC are categorized as direct and indirect techniques [10]. Mode locking is widely used to generate a frequency comb. In this research work, we generate a frequency comb by using mode-locking in a microresonator.

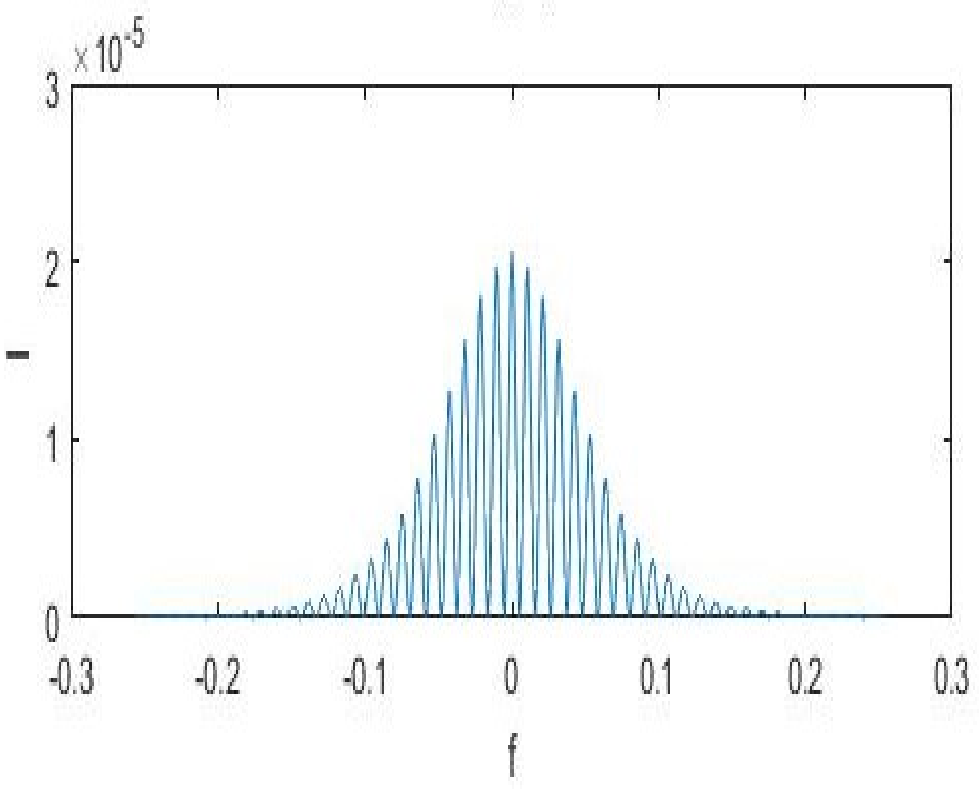

Figure 1.1: A typical Optical frequency comb with equally spaced lines

1.2 Literature review

As mentioned earlier that OFC is a spectrum with uniformly in general spaced lines or frequency components, that resembles with a light frequency ruler. This depicts a broad optical spectrum, with millions of tiny optical comb teeth visible when magnified. Ac-

cording to Fourier transform properties if there are evenly separated lines in the frequency domain, we have a flawlessly spaced train of optical pulses in the time domain and vice versa.The OFC can be produced by a variety of means, including mode-locked lasers stabilizing the pulse train, four waves mixing in a non-linear medium, and so on [12].

In some recent works, OFC spectroscopy with quantum-noise is used. In this continuous wave, the laser spectroscopy technique is used. The technique's sensitivity can be increased by using modulation techniques to transfer the signal to audio [13,14] or radio frequencies [15], which reduces technical noise. The same can be done by using the enhancement in the external cavity that lengthens the interaction length of light and consequently the absorption signal [16,17]. Hajime Inaba et.al. invented a fiber-based OFC using mode-locked laser and reverse pumping. It consists of Er fiber oscillator, a highly non-linear fiber (HNLF), an f CEO detection part, amplifiers, and a beat detection part [18]. It has the highest signal-to-noise ratio (SNR) for an f CEO beat signal as a fiber-based frequency comb. Furthermore, the superior f CEO beat allows us to conduct the longest continuous measurement of optical frequencies.

J. Millo et.al. shows how to create a low-noise microwave signal using a fiber-based mode-locked laser onto an ultrastable optical cavity [21]. In 2022, the Integrated Lithium Niobate modulator-based flat OFC generator has been developed [31].A dual-mode microcavity laser also develops the flat optical frequency [34]. Anatoliy A. Savchenkow et al. used the four-wave mixing method to create a tunable monolithic OFC. Four-wave mixing generates frequency comb in a crystalline calcium fluoride whispering gallery mode resonator.Integer number of free spectral ranges cause the frequency comb spacing. A good and extensive diversity of optical combs are observed under realistic situations [26]. Alongside the experimental work a good amount of theoretical work has also been done. Using the Lugiato-Lefever equation and coupled-mode theory, Tobias Hansson et al. analyzed the frequency comb. Microresonators are used to generate frequency comb, although the same study can be applied to fiber-ring resonators. High intracavity power is observed in the results [27]. In this current age, atomic clocks are used in a variety of applications such as GPS-based communication, ultraviolet, and infrared spectroscopy, microwave waveform creation, research, and industry. The importance of the atomic clock is growing by the day. Actually, OFC works like an atomic clock gear [25].

1.3 Motivation

Till date huge research has been done on modes of light in microresonator and optical frequency comb in a microresonator. Noise has an important role in any system, so for OFC. Depending on relative phase the initial noise (even very small) can create a significantly large pulse. The role of noise on the generation of OFC has not been widely explored. In our investigation, we study the effects of noise on optical frequency comb generation in a microresonator which is based on vertical cavity surface emmiting laser (VCSEL). The following are the objectives of our investigation.

1.4 Objectives

The objectives of our investigation are to study

1. The effect of noise on optical frequency comb generated in a VCSEL based microresonator cavity.

2. The variation of the optical frequency comb with wavelength.

Chapter 2

Fundamentals of OFC in microresonator

In this chapter we discuss the fundamental concepts of the items, phenomena and method that has been used in this thesis.

2.1 Methodology

We consider a VCSEL based microresonator cavity. The VCSEL contains a Graphene saturable absorber (GSA). We first generate a localized structure of light pulse named 'cavity soliton' in the microresonator. The frequency domain presentation of the cavity soliton is the OFC. To overcome the cavity loss and keep the cavity soliton 'alive,' a frequency selective feedback system is used. The following complex Ginzburg-Landau equation (CGLE) describes our system, which consists of VCSEL with GSA and coupled with selective frequency feedback:

$$\frac{\partial E}{\partial t} = [-(1 - i\theta) + \frac{\mu(1 - i\alpha)}{1 + g(E)^2} - \frac{\gamma(1 - i\beta)}{1 + g(E)^2 + \alpha_{ns}} + i\Delta]E + F \tag{2.1}$$

Where,

E is the electric field of the photon, μ & γ are pumping parameters for active and passive materials. α is linewidth enhancement factor for active materials, β is linewidth enhancement factor for passive materials, F is the feedback field, θ is detuning parameter,s is the saturation parameter, α_{ns} is the non-saturable loss, $\iota\Delta$ is the transverse laplacian, g represents the coefficient of saturation of GSA, g=1 stands for semiconductor saturable absorber (SESAM).

This equation (2.1) is too complicated for an analytical solution [28]. This equation can be solved using either the pseudospectral method or the finite difference method. To solve this, we used the Split Step Fourier Method (SSFM), which is a pseudospectral method. This technique was first used in 1973 [29]. This method is relatively simple

to implement because it requires a careful selection of step sizes in z and T so that the desired accuracy maintained.

Step1: Introducing the linear and non-linear operators;

First we write the equation in the form of diffraction operator $\hat{D}$and non-linear operator $\hat{N}$ as follows:

$$\frac{\partial E}{\partial t} = [\hat{D} + \hat{N}]A \tag{2.2}$$

where,

$$\hat{D} = -(1 - \iota\theta) + \iota\Delta + F \tag{2.3}$$

$$\hat{N} = \frac{\mu(1 - \iota\alpha)}{(1 + g(E)^2)} - \frac{\gamma(1 - \iota\beta)}{1 + sg(E)^2 + \alpha ns} \tag{2.4}$$

$\hat{D}$ is a linear operator, and $\hat{N}$ is a non-linear operator.

Step2: By assuming that the dispersive and non-linear effects behave separately when the optical field travels over a short distance h, the SSFM arrives to an approximation of the answer. There are two steps in the propagation process from z to z+h:-

Firstly, diffraction acts alone, and $\hat{N}$=0; Therefore,

$$\frac{\partial E}{\partial t} = \hat{D}E \tag{2.5}$$

We integrate it from limit $E(z, T)$ to $E(z, T + h)$ as

$$\int_{E(z,T)}^{E(z,T+h)} \frac{\partial E}{E} = \hat{D} \int_{T}^{T+h} \delta T \tag{2.6}$$

$$E(z, T + h) = E(z, T) \exp h\hat{D} \tag{2.7}$$

Secondly, non-linearity acts alone and $\hat{D}$=0; So,

$$\frac{\partial E}{\partial t} = \hat{N}E \tag{2.8}$$

We now integrate it from limit $E(z,T)$ to $E(z,T+h)$

$$\int_{E(z,T)}^{E(z,T+h)} \frac{\partial E}{E} = \hat{N} \int_{T}^{T+h} \delta T \tag{2.9}$$

$$E(z,T+h) = E(z,T) \exp h\hat{N} \tag{2.10}$$

Now, combining the equations (2.7) and (2.10); we get

$$E(z,T+h) = \exp\left(h\hat{D}\right) \exp\left(h\hat{N}\right) A(z,T) \tag{2.11}$$

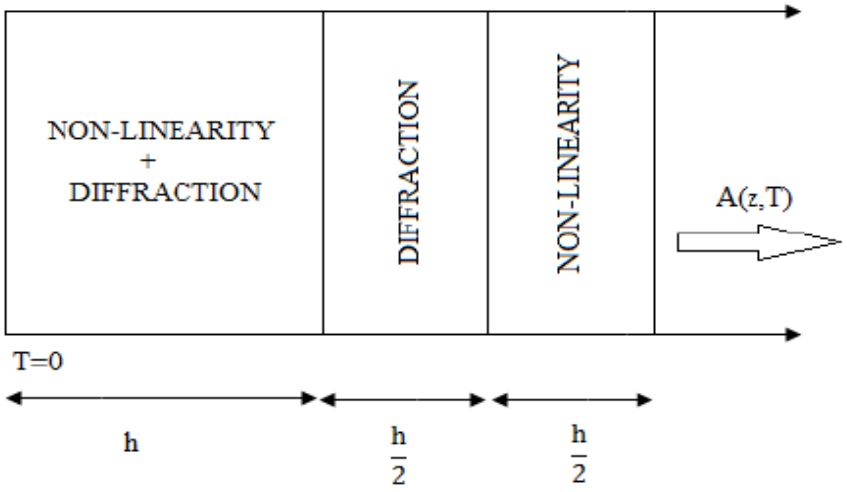

Figure 2.1: Schematic demonstration of the symmetrized split-step Fourier method. (Image concept: - Nonlinear fiber optics 4th edition, Govind P Agarwal, page 43)

In fourier domain exp(h$\hat{D}$) can be written as:

$$\exp\left(h\hat{D}\right) B(z,T) = F_T^{-1} \exp\left[h\hat{D}(-\iota\omega)\right] FTB(z,T), \tag{2.12}$$

where FT is the Fourier transform operator, and ω is the frequency. $\hat{D}(\iota\omega)$ is taken from equation (2.3) by replacing Δ with $\iota\omega$, ω is the frequency in the Fourier domain $\hat{D}(\iota\omega)$ is

just a number in Fourier space. The use of the FFT algorithm makes the evaluation of equation (2.12) relatively fast. NOw, exact solution of equation (2.2) can be given by

$$E(z+h,T) = \exp\Big[h(\hat{D}+\hat{N})E(z,T)\Big] \tag{2.13}$$

Here, $\hat{N}$ is supposed to be independent of T.

The Baber-Hausdorff formula for two non-commuting operators $\hat{a}$ and $\hat{b}$ can be written as

$$\exp(\hat{a})\exp\Big(\hat{b}\Big) = \exp\bigg(\hat{a}+\hat{b}+\frac{1}{2}[\hat{a}\hat{b}]+\frac{1}{12}[\hat{a}-\hat{b},[\hat{a},\hat{b}]+....]\bigg) \tag{2.14}$$

where $[\hat{a},\hat{b}]$ =$\hat{a}\hat{b}$-$\hat{b}\hat{a}$

We use the above equation with $\hat{a}$ =h$\hat{D}$ and $\hat{b}$=h$\hat{N}$. The dominant error term is found from two non-commutators as $\frac{1}{2}h^2[\hat{D},\hat{N}]$. Thus SSFM generally ignores the nature of non-commutating operators. The accuracy can be enhanced by rewriting the equation (2.11) as,

$$A(z,T+h) = \exp\bigg(\frac{h}{2}\hat{D}\bigg)\exp\bigg(\int_T^{T+h} N(T')\bigg)\exp\bigg(\frac{h}{2}\hat{D}\bigg)A(z,T) \tag{2.15}$$

Here the effect of non-linearity is included in the middle of the segment (fig 2.1) rather than at the segment boundary. This is a common practice. This is known as the symmetrized split-step Fourier method because of a symmetric form of exponential operators in equation (2.15). This method is well known and has been applied to numerous optical problems [30].

2.2 Soliton

Soliton is a significant and fascinating research issue in various domains, including biology, physics, and chemistry. A soliton is a structure that keeps its shape and size during propagation for a long distance. John Scott Russell was the first to obsrve (in 1834) and suggest this concept after 10 years [32]. During his duty he noticed a heap of water flowing up the head of a boat's bow that continued to travel even after the boat was stopped. For an extended period, the water wave remained unchanged in size and shape.

He gave the wave as 'wave of translation'. Later on these waves are referred as solitary waves. Such waves can be found in other media or disciple too.

A light wave begins to broaden fade after propagation of some distance to dispersion due to diffraction, and loss. Nonlinearity, of the mediummay cause self-phase modulation the contraction of the pulse, self focusing and hence we achieve conservative soliton in a non-linear medium when these two processes (i.e., broadening contraction) balance. If there is a loss in the system, soliton will not be steady. An external gain can compensates this loss during wave propagation, resulting in a stable soliton [33].

Soliton has a particle like nature, thus solitons preserve their shape and size during transit and even after impact [30]. Spatial solitons are formed when self diffraction and self-focusing are balanced. temporal solitons are formed when a group velocity dispersion is balanced by self phase modulation. We know that no practical system can exists in an ideal state, i.e., there are losses in the system. External gain can compensate this loss. Dissipative solitons (DS) are a sort of solitons seen in these types of easy systems [36]. Many biological [37], chemical [33], and physical [38,39] systems exhibit this form of solitons. Dissipative solitons require regular external energy to keep their structure alive. In contrary, the conservative soliton does not require a constant supply of external gain.

Some typical fundamental and higher order soliton profiles are given in fig. 2.2-2.4.

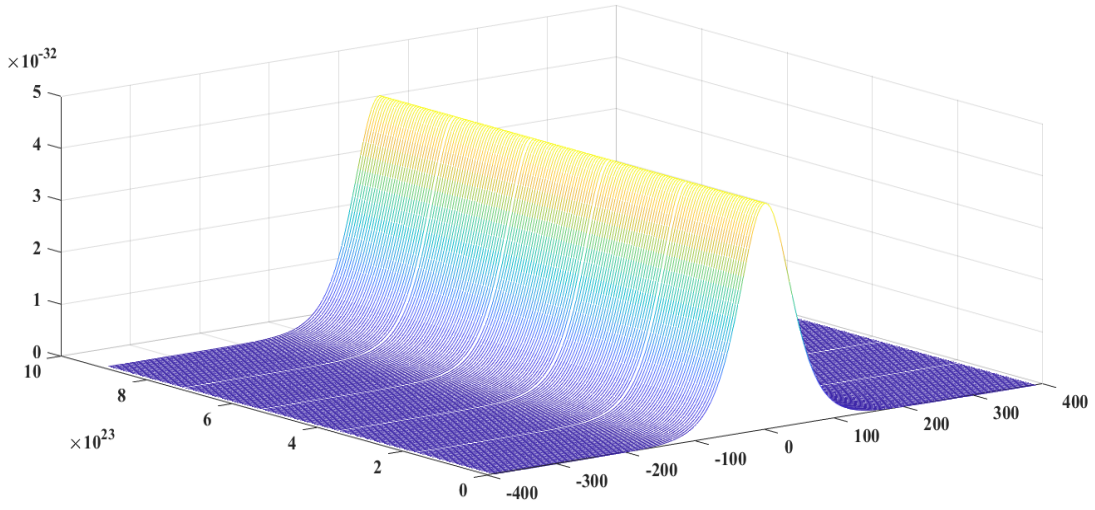

Figure 2.2: 1st order Soliton formation

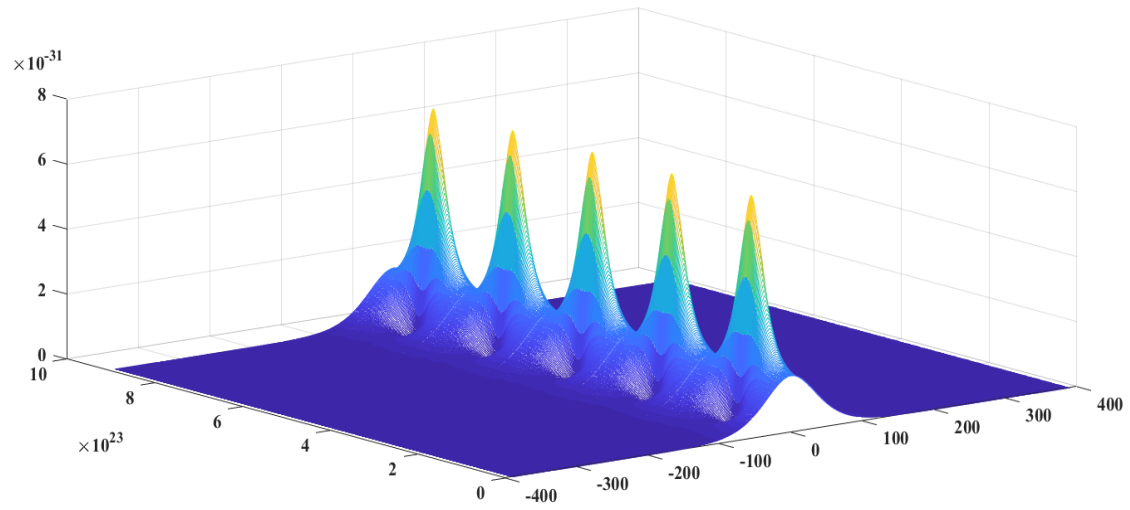

Figure 2.3: 2nd order Soliton formation

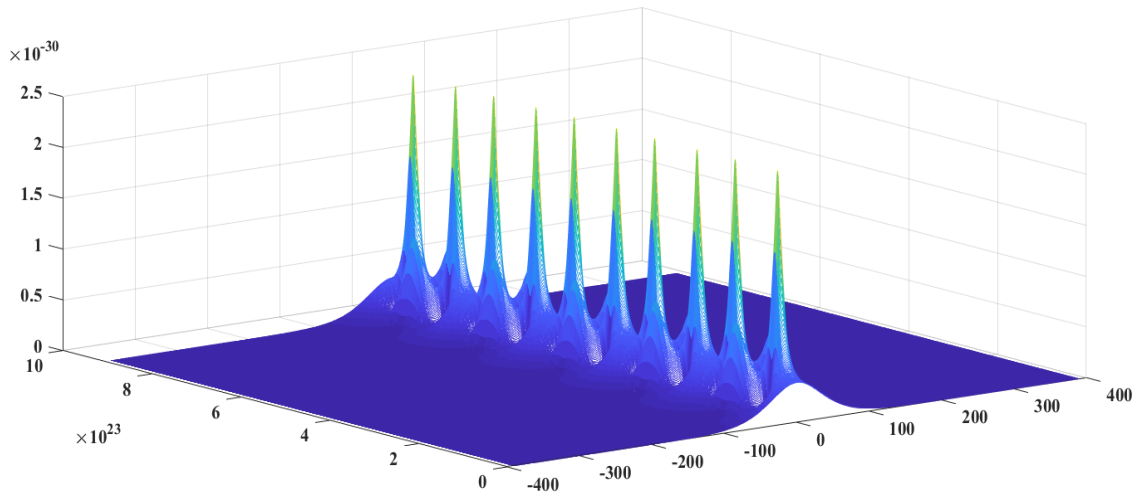

Figure 2.4: 3rd order Soliton formation

The fundamental soliton preserves its shape and size during propagation while the higher order solitons periodically change those.

2.3 Vertical cavity surface emitting laser

Prof. Kenici Igra proposed the invention of vertical-cavity surface-emitting lasers in 1980. These are laser diodes, which emit light in a direction perpendicular to the chip surface. The VCSEL is the most widely used semiconductor laser because of its many advantages, including high output power, low noise operation, lower temperature sensitivity, low threshold currents and high transmission speed with low power consumption [40]. It is

now a days being used commerically too. VCSEL is made up of layers of semiconductor material that are developed on top of one another. Two sets of Bragg mirrors form the microresonator. Between these two mirrors lies the gain medium (active region). Saturable absorber are placed in between the mirrors. Face ID, smart glasses, computer mice, and other laser based devices utilize VCSELs [7].

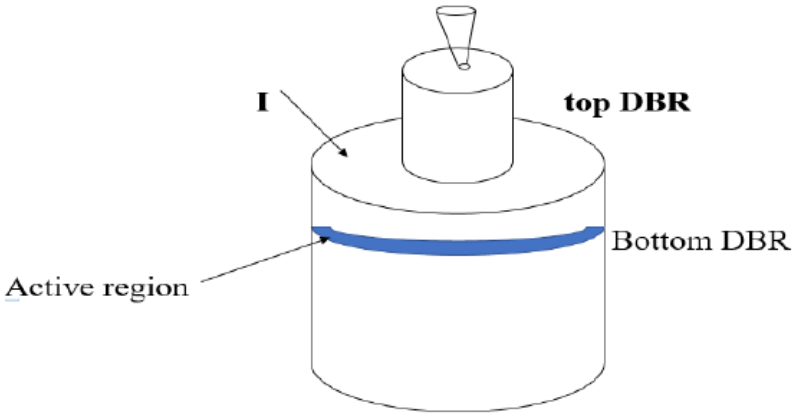

Figure 2.5: Schematics of vertical cavity surface emitting laser

Here we use VCSEL as a host of cavity soliton that in turn gives rise to the OFC.

2.4 Mode locked laser

Inside a laser cavity many modes can be created. When the laser operates at a particular mode we get a mode-locked laser. Laser mode-locking is a technique for producing ultra-short pulses. Mode-locking can be active (optical modulator) or passive (non-linear material, such as a saturable absorber). In active mode-locking process a standing wave electro-optic modulator is inserted into the laser cavity. The periodic modulation of the resonator is used in this technique [41]. When the modulation is synced with the resonator round trips, ultra-short pulses are generated. These ultra-short pulses are usually of the order of picoseconds.

The most basic mode-locked laser generally uses a linear cavity that contains a semiconductor saturable absorber mirror (SESAM). A SESAM is made up of a reflector with a quantum well absorber layer on the front face. This layer is used to hide the reflector's front face. The quantum wells absorb light at the laser wavelength. When the

optical intensity is high enough, the quantum wells can be temporarily depleted and become transparent. Thermal relaxation and recombination processes regain absorption only after a high-intensity light pulse strikes the SESAM. The recovery time of a SESAM is usually of the order of picoseconds. The recovery time is a key element to design a mode-locked laser. Mode-locked lasers with a SESAM usually have great self-starting characteristics and high repeatability [3].

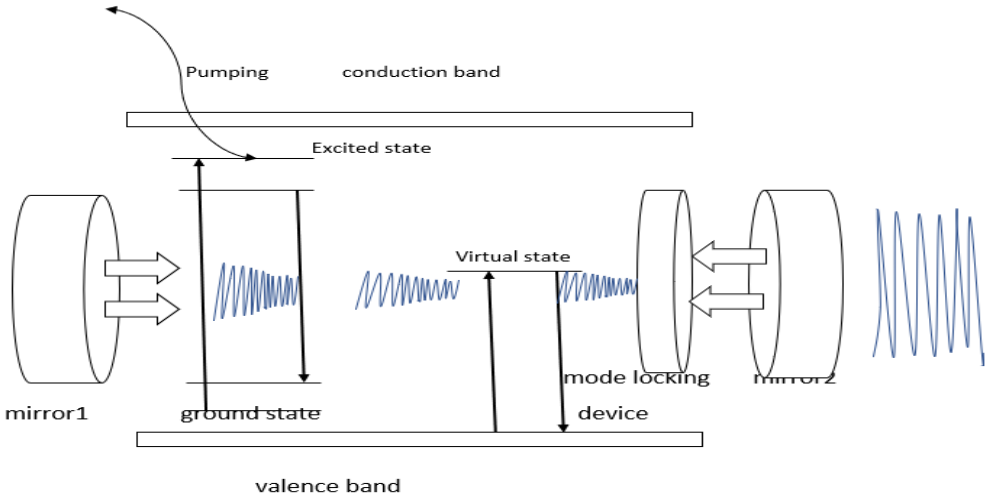

Figure 2.6: A typical scheme for generation of optical frequency comb using mode locked laser

2.5 Frequency selective feedback

Our system consists of VCSEL coupled with an external frequency-selective feedback (FSF). A FSF operates, as the name implies, in a particular frequency range, thus lowers the laser threshold only to a narrow frequency range [43].

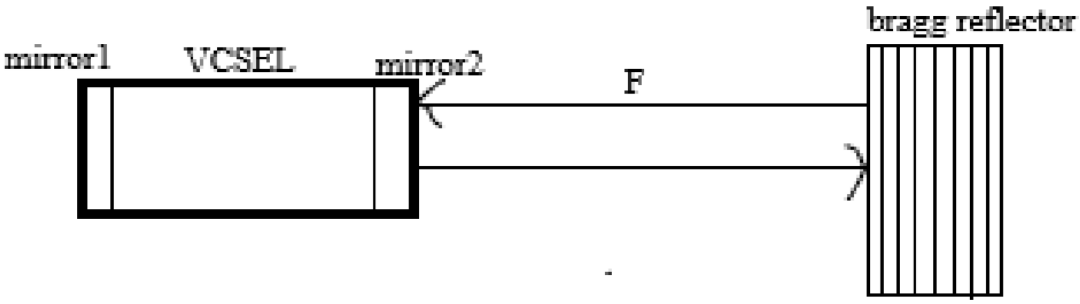

Figure 2.7: Schematic of the microcavity coupled with the FSF

With the knowledge of all these component and methdology we now proceed to find the OFC via cavity soliton inside the VCSEL based microresonator.

Chapter 3

Results and Discussion

3.1 Results

In the very begining we generate cavity soliton in the VCSEL based microresonator with saturable absorber and coupled with a FSF. Importantlly, these cavity solitons are spatial soliton (localized in space), therefore, the corresponding OFCs are spatial OFC instead of temporal OFCs. Following are the results without noise. Here an input beam is injected in the microcavity. The spatial profile and the frequency and time domain profile of the beam is given in (fig.3.1). We show a typical evolution of real and imaginary parts in fig.3.2. Fig. 3.3 depicts the evolution of a pair of cavity solitons from a single input beam. Such solitons are generated where the self-diffraction of the beam is counter balanced by the self-focusing of the beam (by virtue of nonlinearity) and the system loss is compensated by FSF.

Throughout this thesis, unless mentioned otherwise, we used the following values of parameter

$\theta = 1.7$, $\mu = 1.37$, $\alpha = 3.2$, $\gamma = 0.5$, $\beta = 0.3$, $s = 10$, $G = 1.37$, for GSA; G=1 for SESAM; $\lambda = 0.5$, $\sigma = 0.3$, $\Omega = 1.7$ [42].

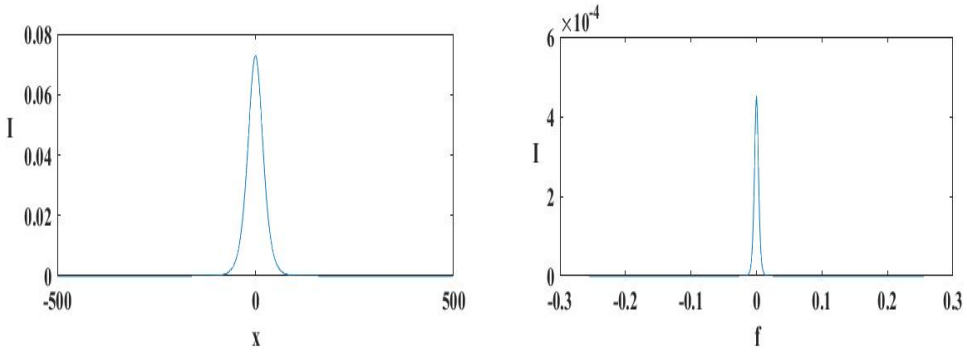

Figure 3.1: The input beam profile and its profile in frequency domain.

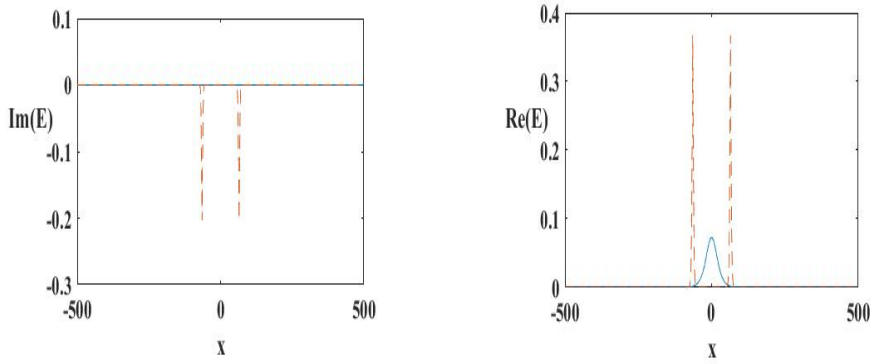

Figure 3.2: Evolution of real and imaginary parts of the beam in the microcavity.

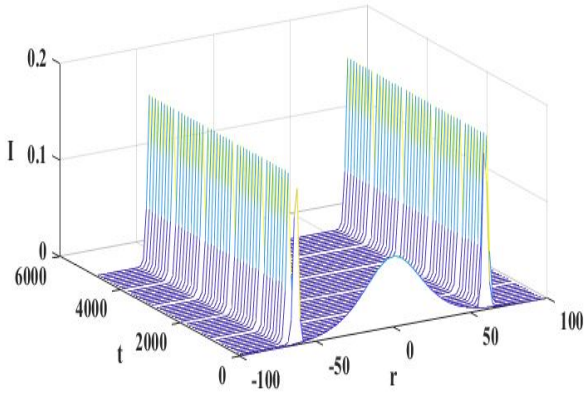

Figure 3.3: The evolution of the beam into two cavity soliton in the microcavity.

The cavity soliton thus generated, is now portrayed in spatial frequency domain. Fig. 3.4(a) shows the 2D profile of the input beam (blue solid line) as well as the generated cavity soliton pair (red dotted line). Fig. 3.4(b) is the corresponding OFC in spatial frequency domain.

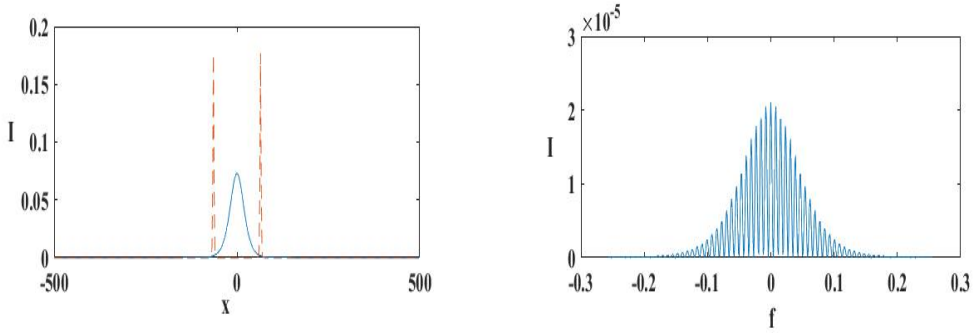

Figure 3.4: (a) The output beam and output cavity soliton pairs (b) the OFC.

3.1.1 Effect of signal to noise ratio on broad spectrum optical frequency comb:

We now investigate the optical frequency comb with noise using the above results. We investigated optical frequency comb with average white Gaussian noise with an average noise range of 0.5. We consider different values of SNR and plot the spatial OFC.

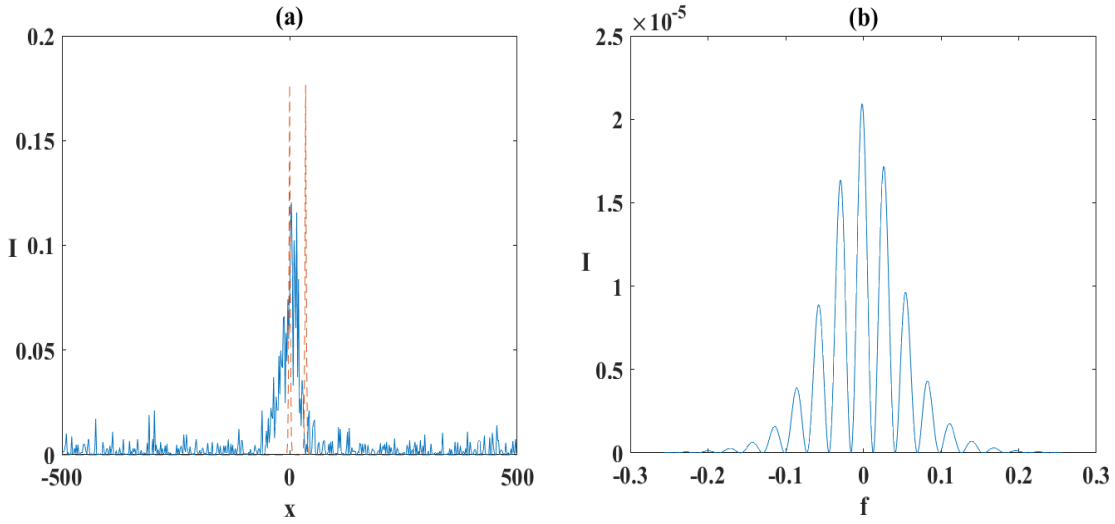

Figure 3.5: (a) The generation of a pair of cavity solitons(tall thin dotted lines) from an input signal(short blue-white profile) and (b) the corresponding OFC. Here the SNR is 26.5.

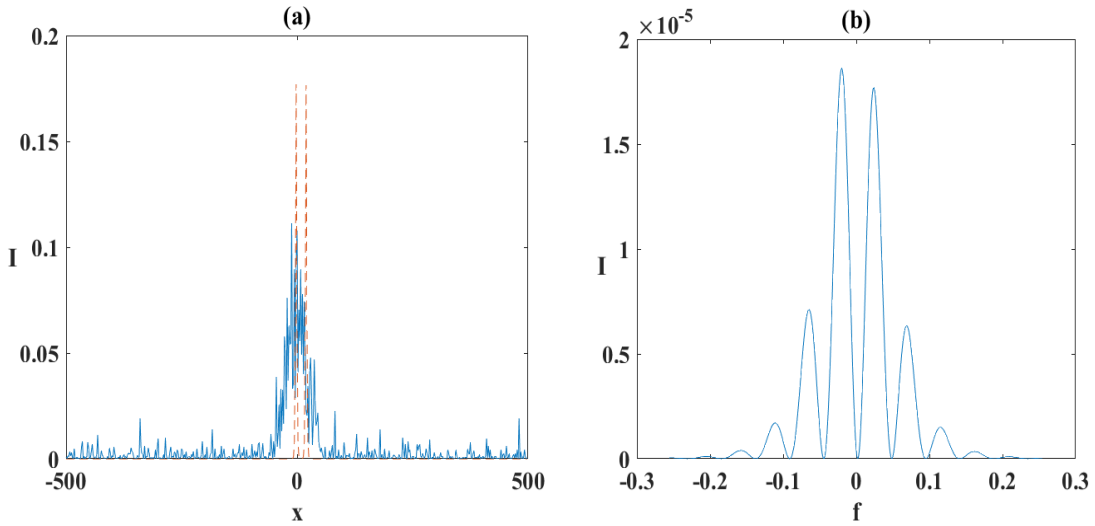

Figure 3.6: Same as fig. 3.5, but for SNR is 27.

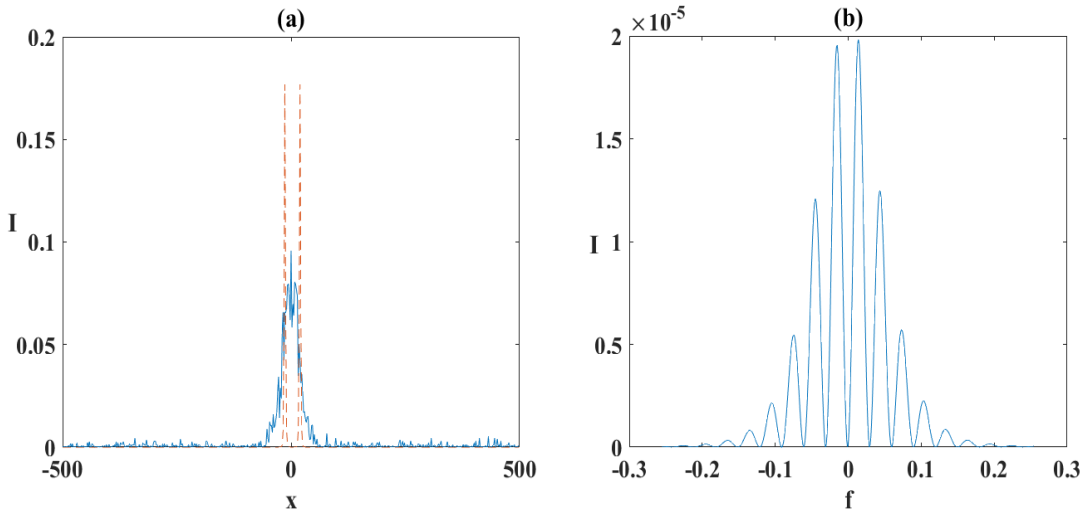

Figure 3.7: Same as fig. 3.5, but for SNR is 31.5.

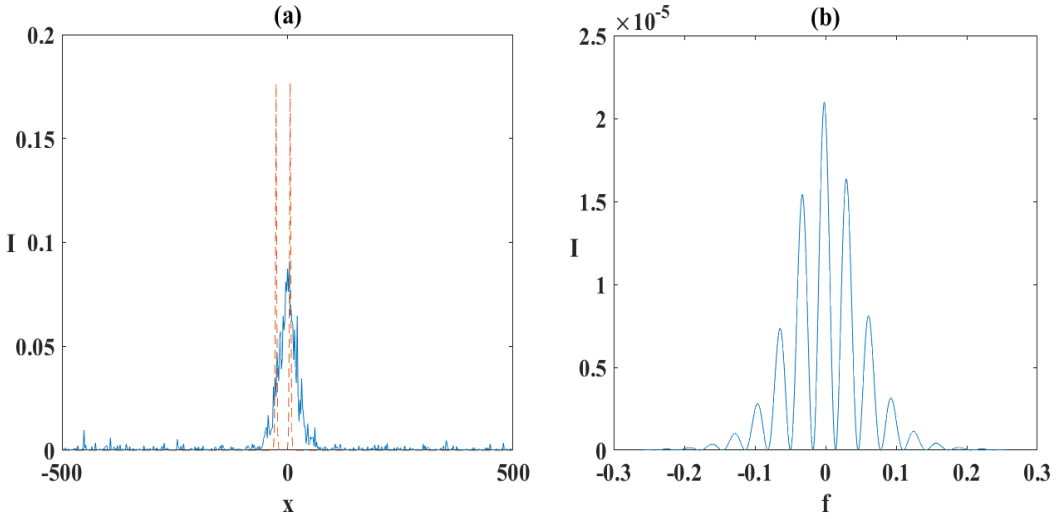

Figure 3.8: Same as fig. 3.5, but for SNR is 32.5.

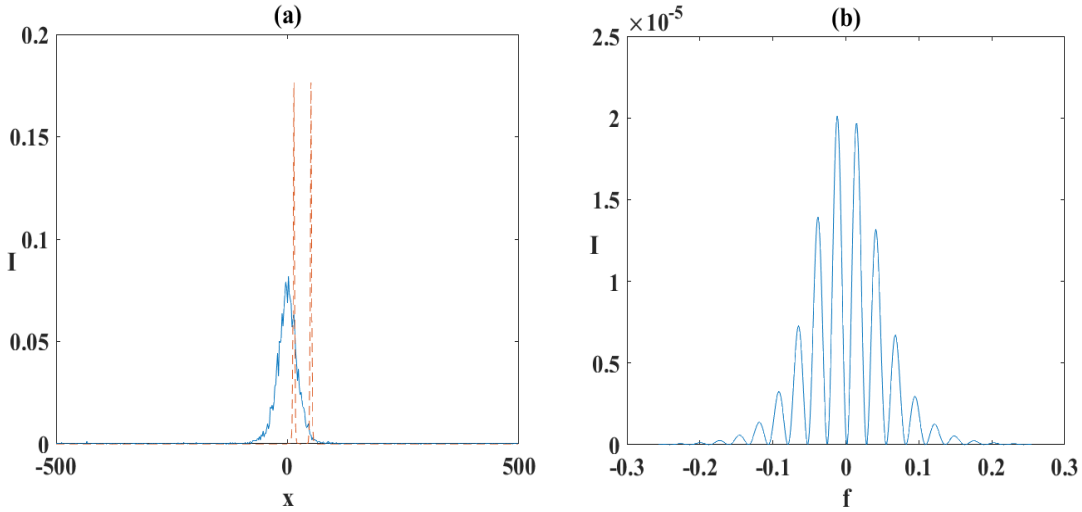

Figure 3.9: Same as fig. 3.5, but for SNR is 41.

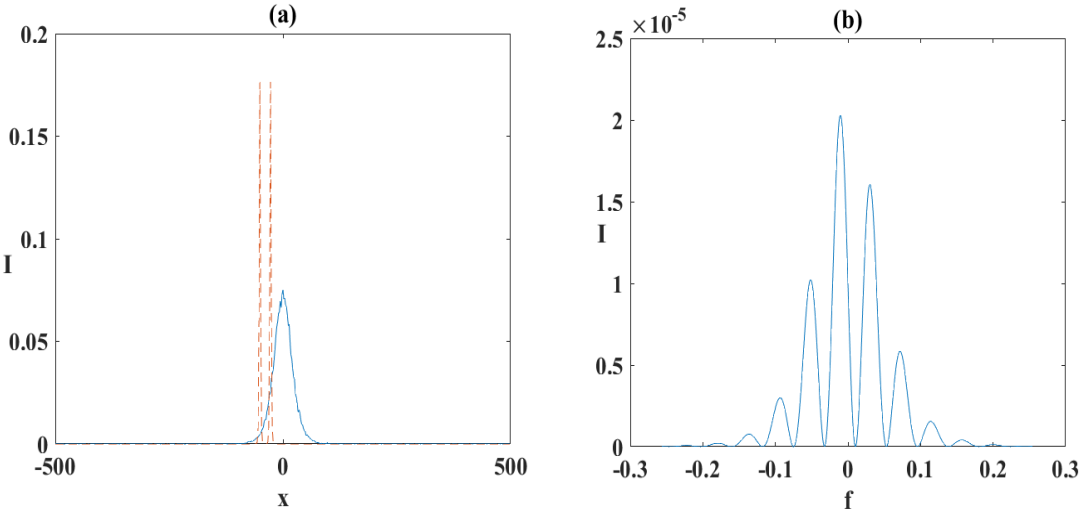

Figure 3.10: Same as fig. 3.5, but for SNR is 49.5.

Fig. 3.5 to 3.10 show that OFC can be generated with S/N as small as 26.5. As S/N ratio increases the number of teeth in the OFC first increases then decreases.

3.1.2 Effect of signal to noise ratio on optical frequency comb with narrow teeth:

We find OFC with large number of teeth, i.e., the narrow teeth. mainly for large S/N ratios give rise to such good quantity OFC. Following are the OFCs at different S/N ratio ranging from 32 to 76.

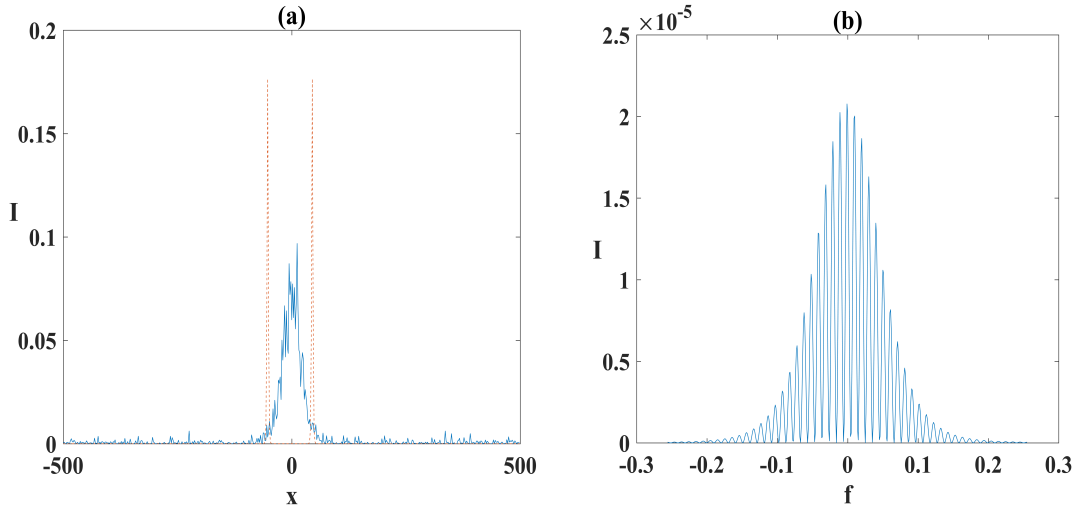

Figure 3.11: (a) The generation of a pair of cavity solitons(tall thin dotted lines) from an input signal(short blue-white profile) and (b) is the corresponding OFC. Here the SNR is 32.

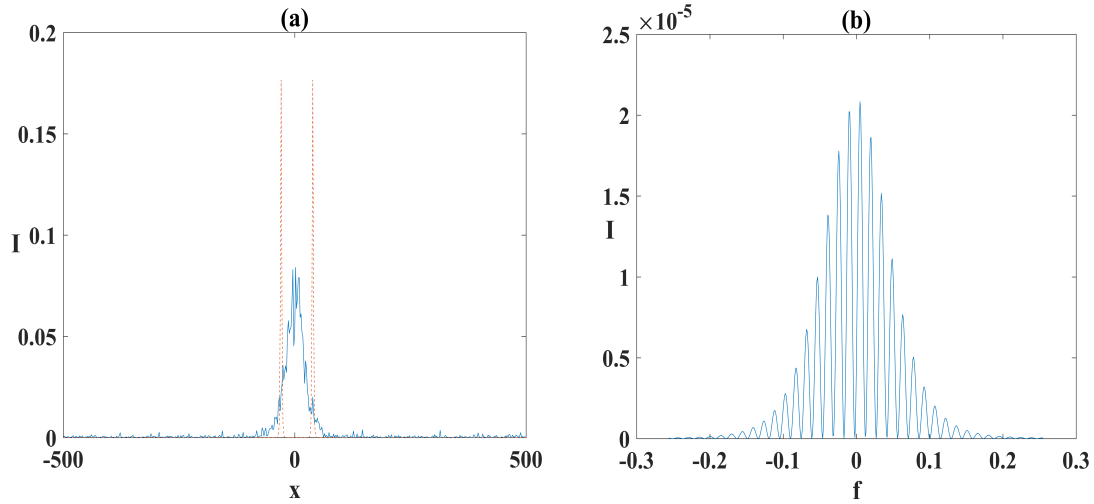

Figure 3.12: Same as fig. 3.11, but for SNR is 34.

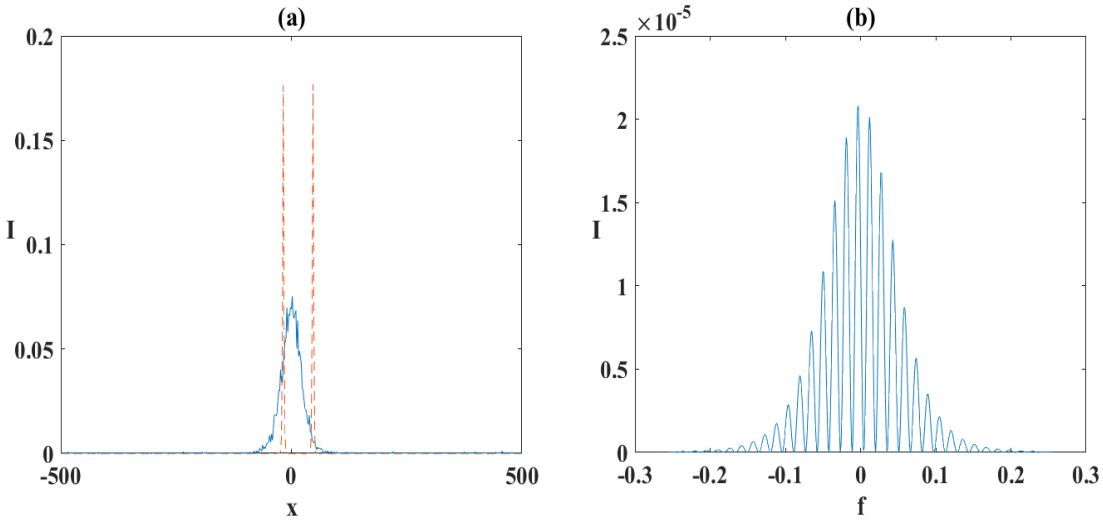

Figure 3.13: Same as fig. 3.11, but for SNR is 40.

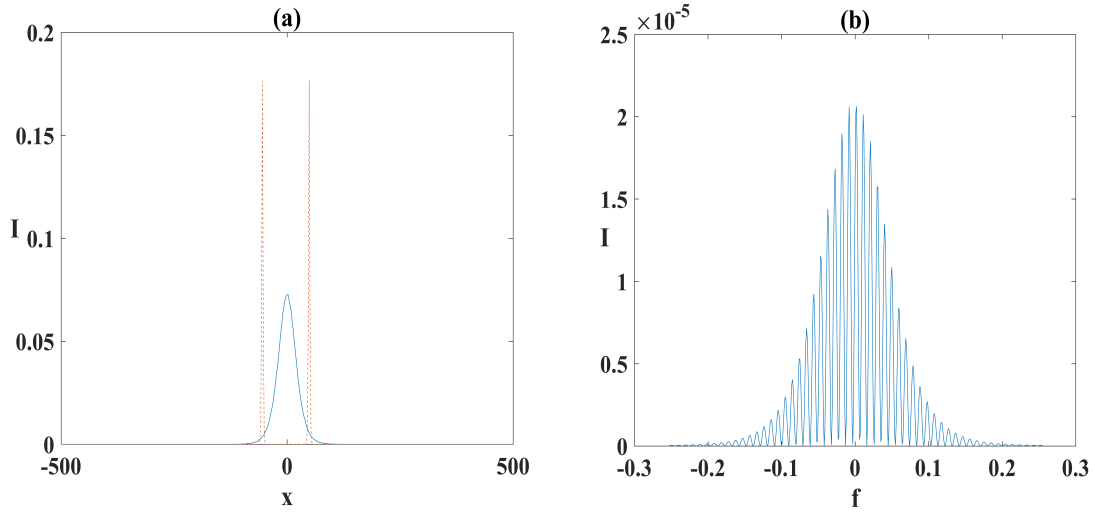

Figure 3.14: Same as fig. 3.11, but for SNR is 58.5.

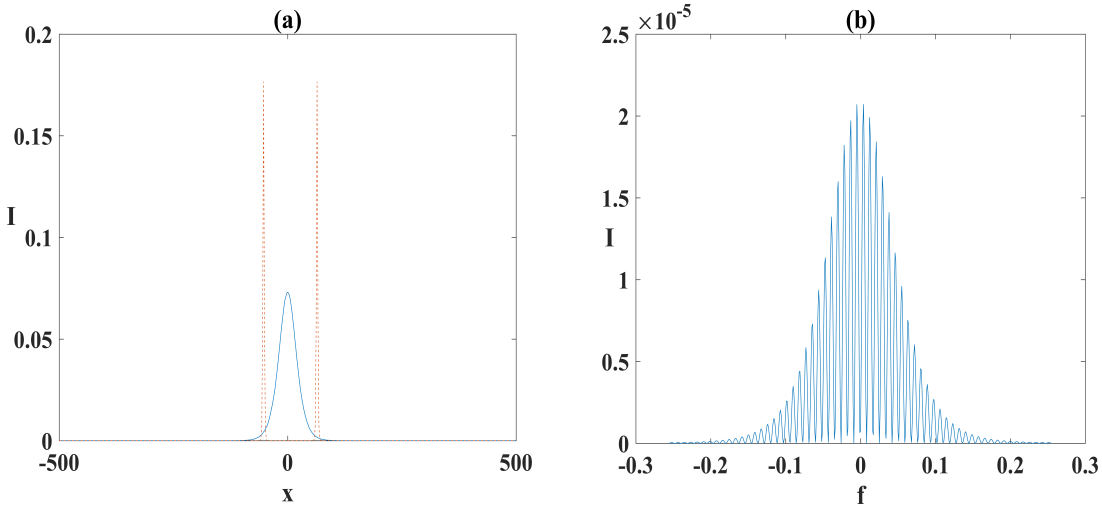

Figure 3.15: Same as fig. 3.11, but for SNR is 66.

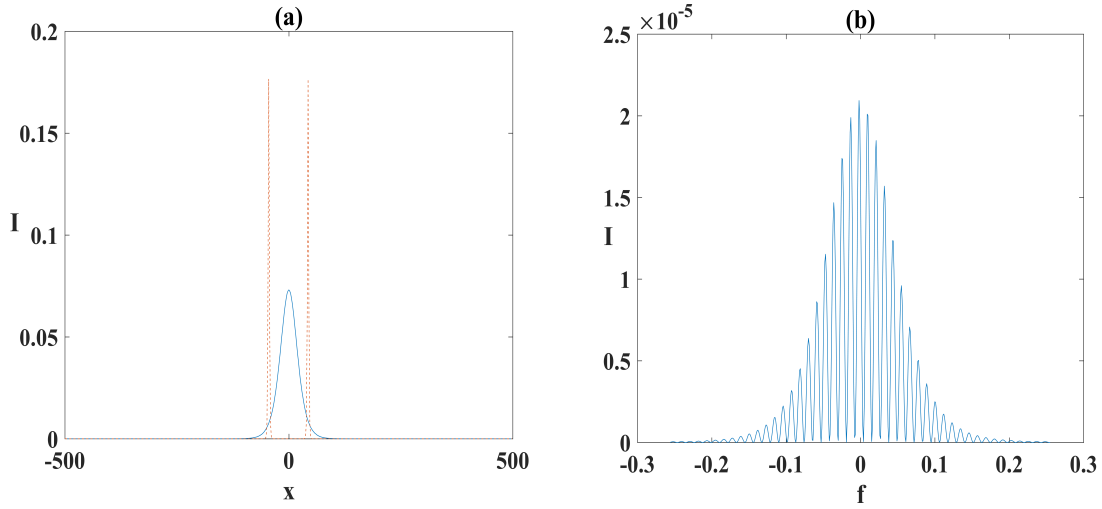

Figure 3.16: Same as fig. 3.11, but for SNR is 69.

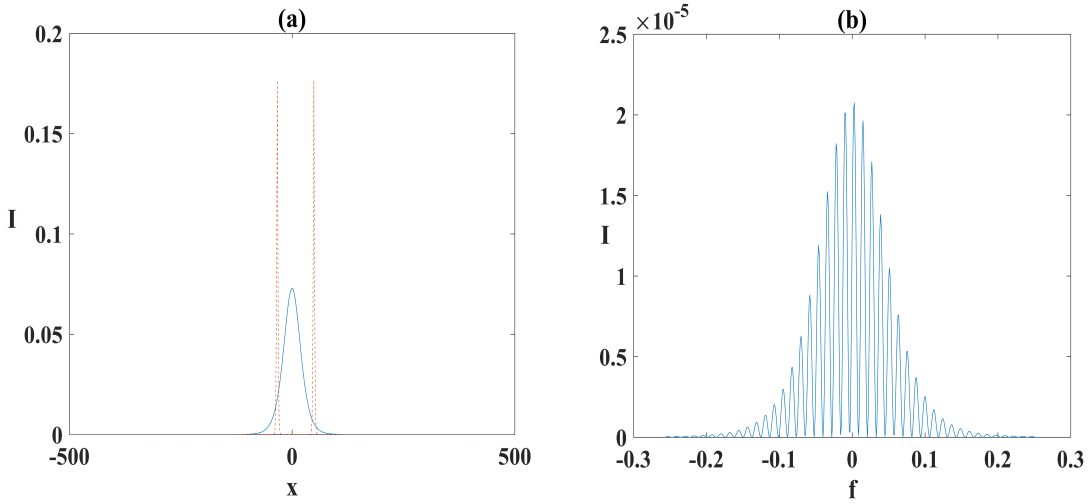

Figure 3.17: Same as fig. 3.11, but for SNR is 72.5.

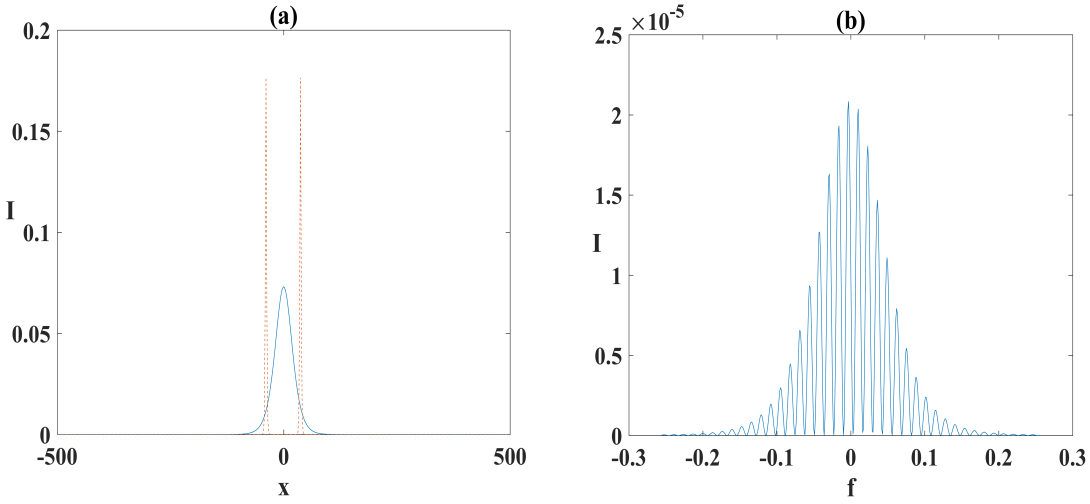

Figure 3.18: Same as fig. 3.11, but for SNR is 74.

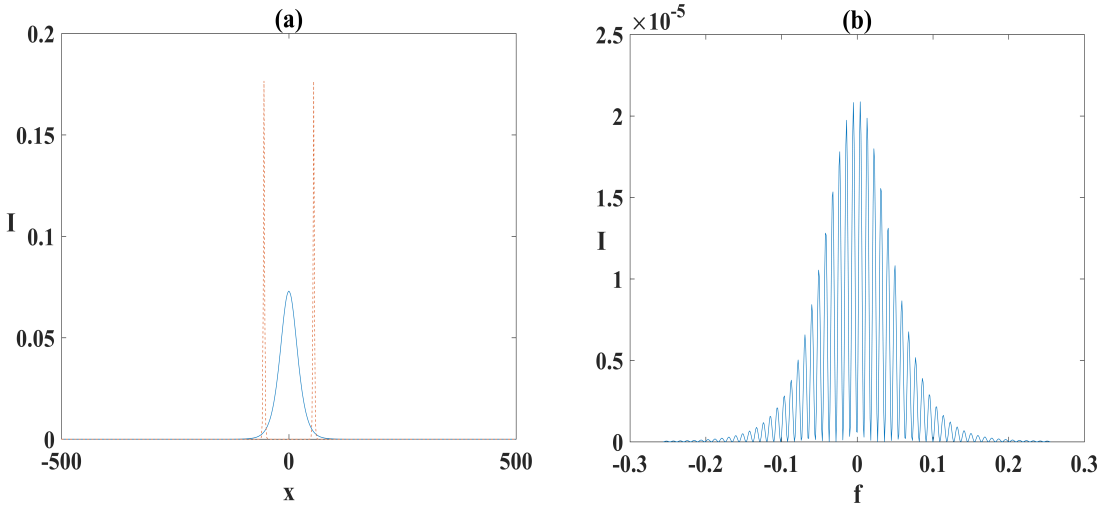

Figure 3.19: Same as fig. 3.11, but for SNR is 76.

From fig. 3.11 to 3.19 it has been observed that with increasing S/N ratio the cavity solitons become more distinct. The corresponding OFC in this large S/N ratio range are more precise than the previous set given in fig. 3.5 to 3.10.

3.1.3 Effect of signal to noise ratio on poor optical frequency comb:

Not all S/N ratio can generate a good OFC. Some example are given here.

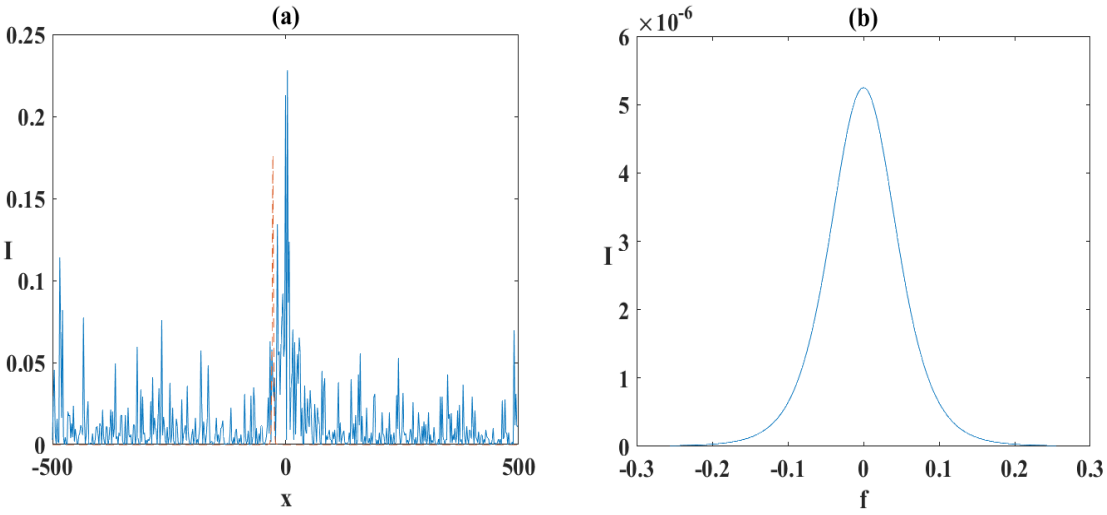

Figure 3.20: (a) The generation of a single cavity soliton(tall thin dotted lines) from an input signal(short blue-white profile) and (b) is the corresponding profile in spatial frequency domain. Here the SNR is 20.5.

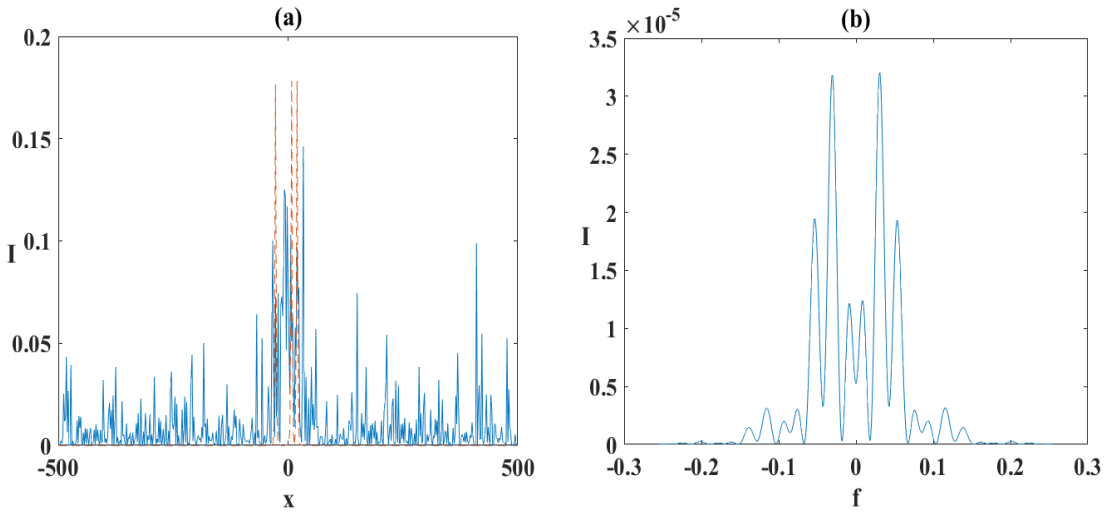

Figure 3.21: (a) The generation of a three of cavity solitons(tall thin dotted lines) from an input signal(short blue-white profile) and (b) is the corresponding OFC. Here the SNR is 21.

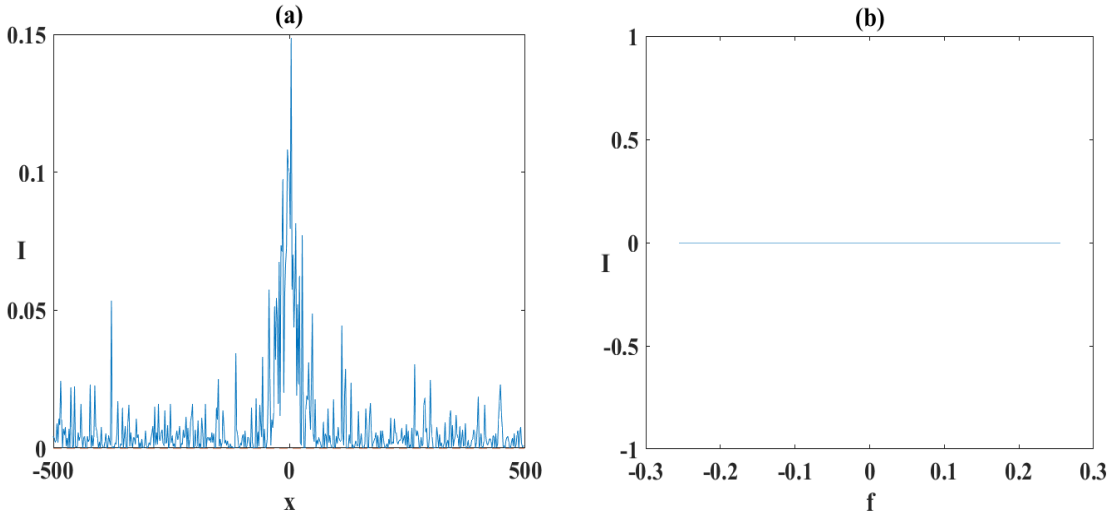

Figure 3.22: For the signal to noise ratio(S/N) 23 no cavity soliton is generated from the input signal(short blue-white profile) and (b) so no OFC is generated.

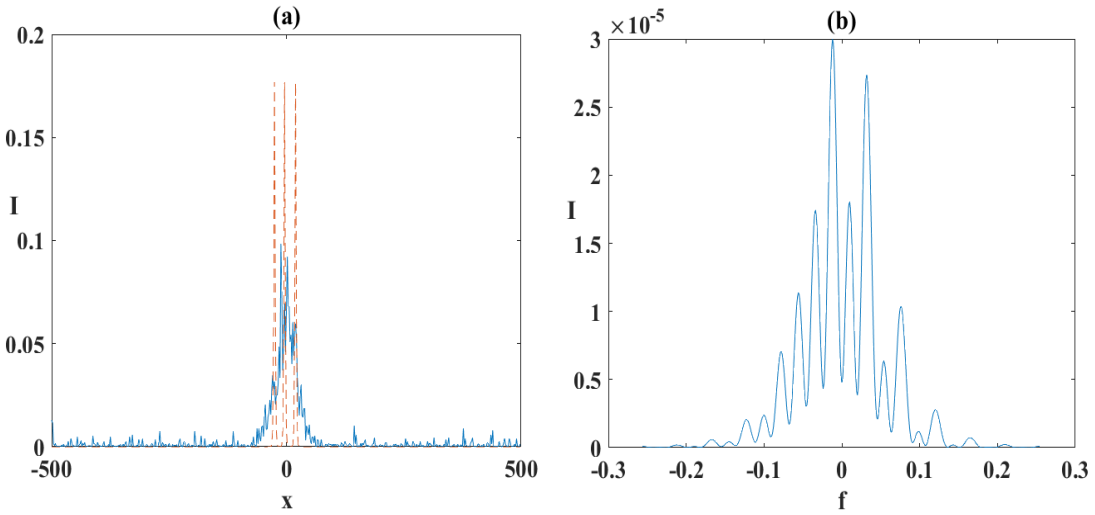

Figure 3.23: (a) The generation of a three of cavity solitons(tall thin dotted lines) from an input signal(short blue-white profile) and (b) is the corresponding OFC. Here the SNR is 30.

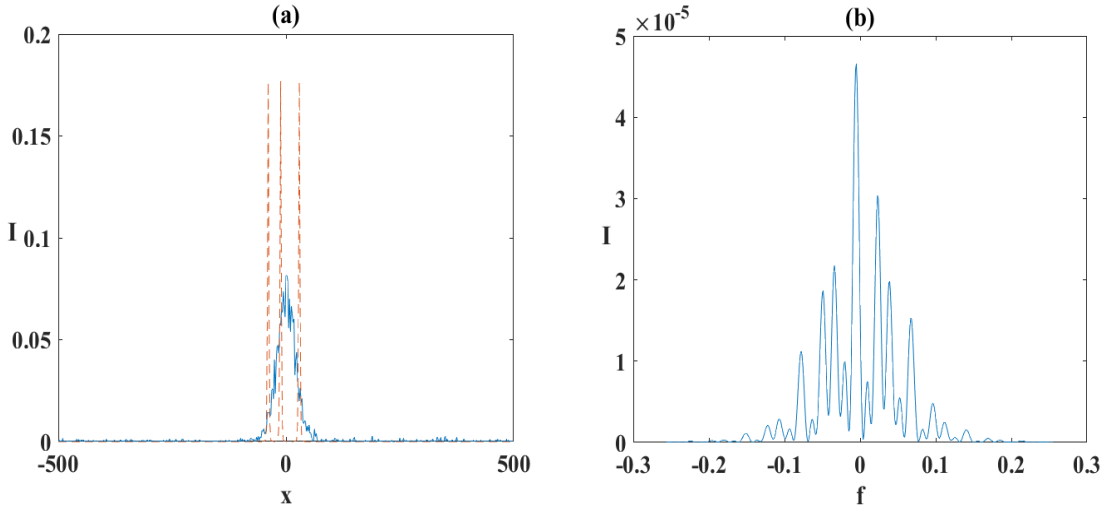

Figure 3.24: (a) The generation of a three of cavity solitons(tall thin dotted lines) from an input signal(short blue-white profile) and (b) is the corresponding OFC. Here the SNR is 35.5.

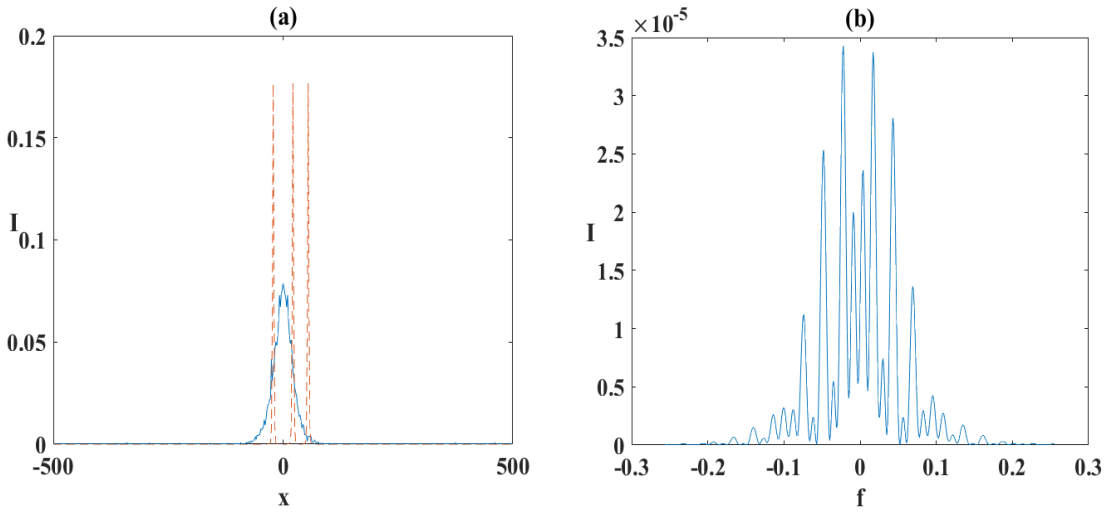

Figure 3.25: Same as fig. 3.23 3.24, but for the SNR is 41.5.

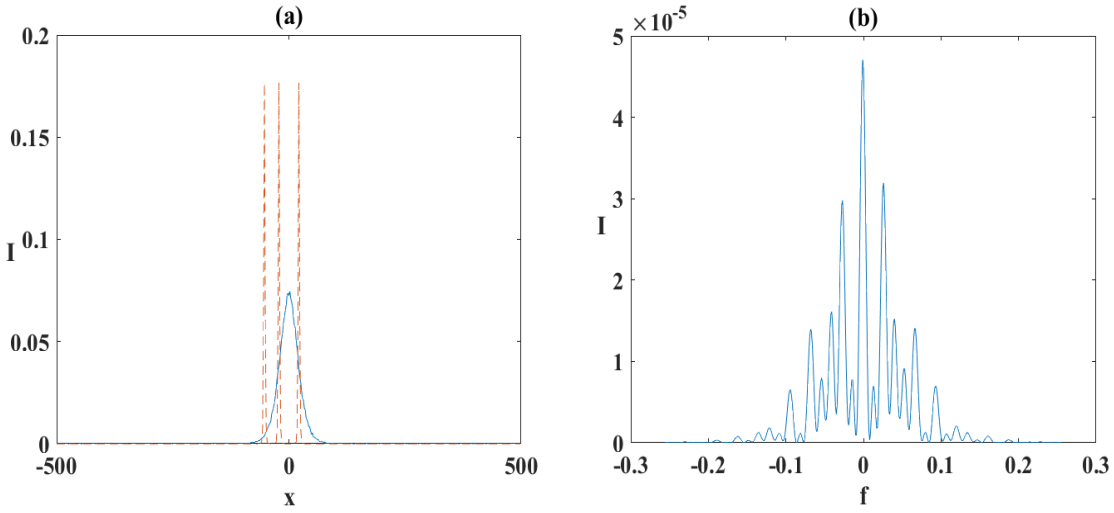

Figure 3.26: Same as fig. 3.23, but for the SNR is 49.

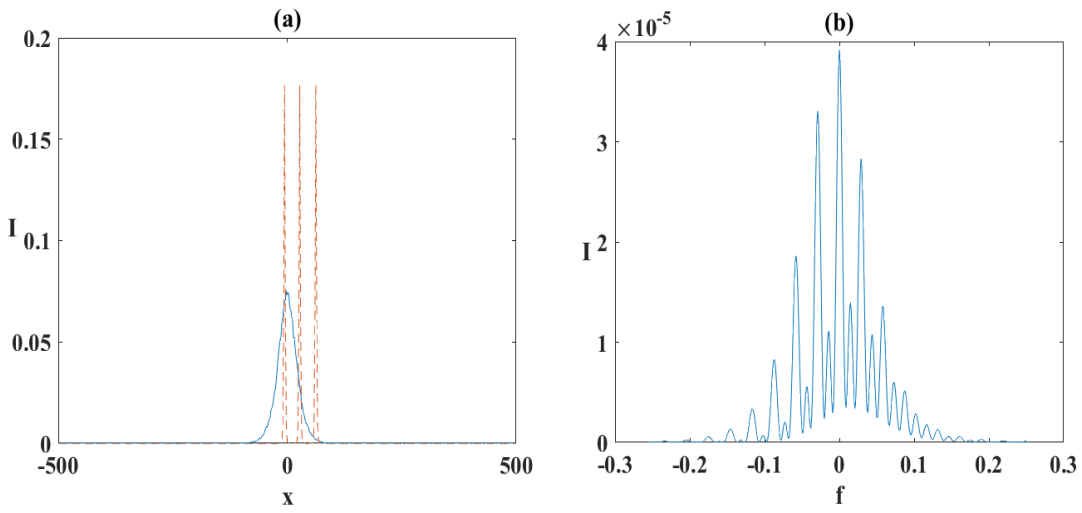

Figure 3.27: Same as fig. 3.23, but for the SNR is 50.5.

Till now, whatever OFC have demonstrated has been found in an operating wavelength 981nm. It is benificial to study the OFC in optical communication wavelengths namely 1330nm, 1550nm and 2000nm. Generally VCSEL (based on which we generated OFC) operates in the wavelength range of 750-980nm [44] whoever longer wavelengths particularly 1330nm, 1550nm and even further higher wavelength are supported by VCSEL. In the coming section we explore OFC in the above mentioned optical communication wavelength. We also studied OFC in 2000nm i.e., in infrared region.

3.2 Optical frequency comb with different wavelength:

We find OFC and the effect of noise on it at the most used optical communication wavelength, namely 1330nm.

3.2.1 Optical frequency comb at wavelength 1330nm:

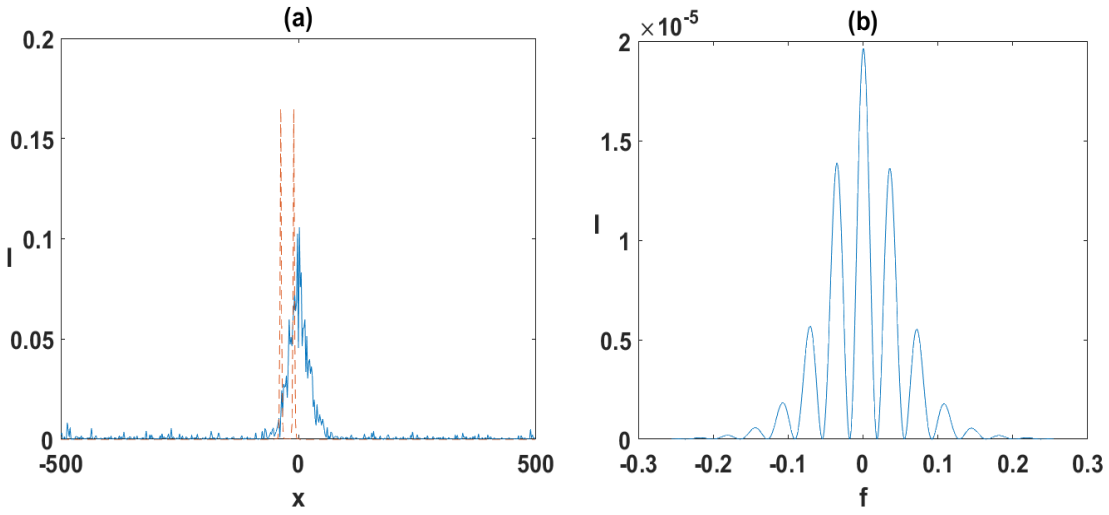

Figure 3.28: (a) The generation of a pair of cavity solitons(tall thin dotted lines) from an input signal(short blue-white profile) and (b) is the corresponding OFC. Here the SNR is 32.

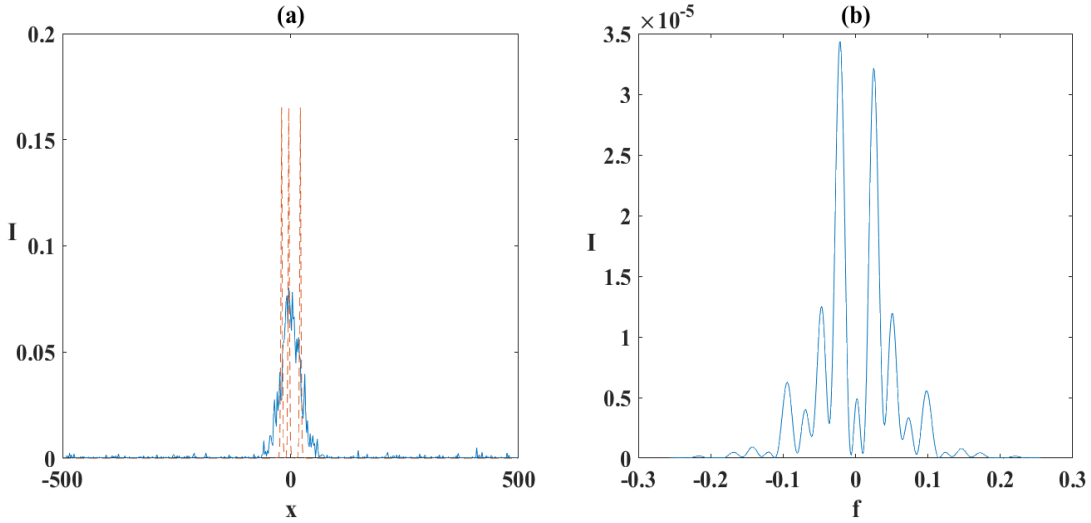

Figure 3.29: (a) The generation of a three cavity solitons(tall thin dotted lines) from an input signal(short blue-white profile) and (b) is the corresponding OFC. Here the SNR is 34.

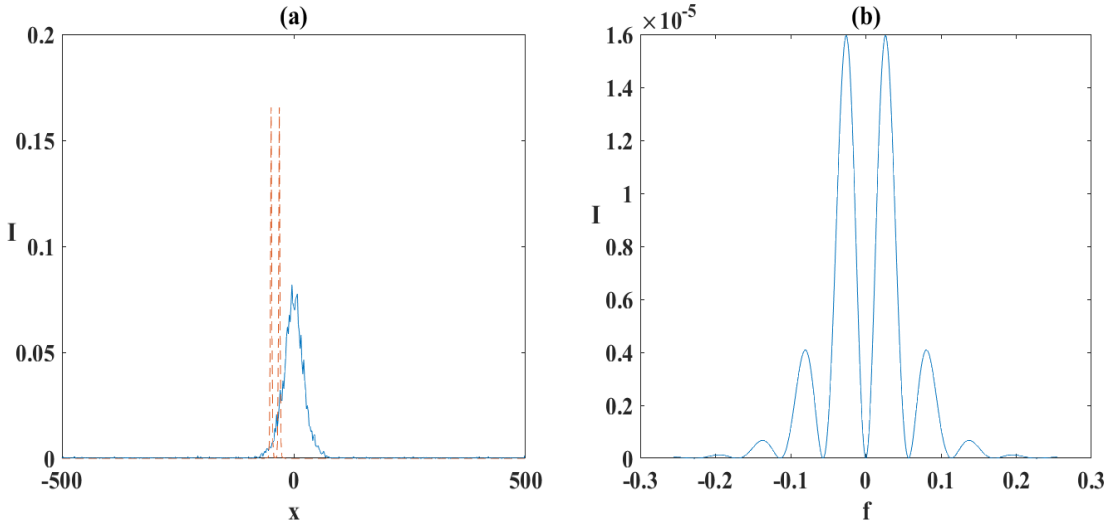

Figure 3.30: Same as fig. 3.28, but for the SNR is 40.

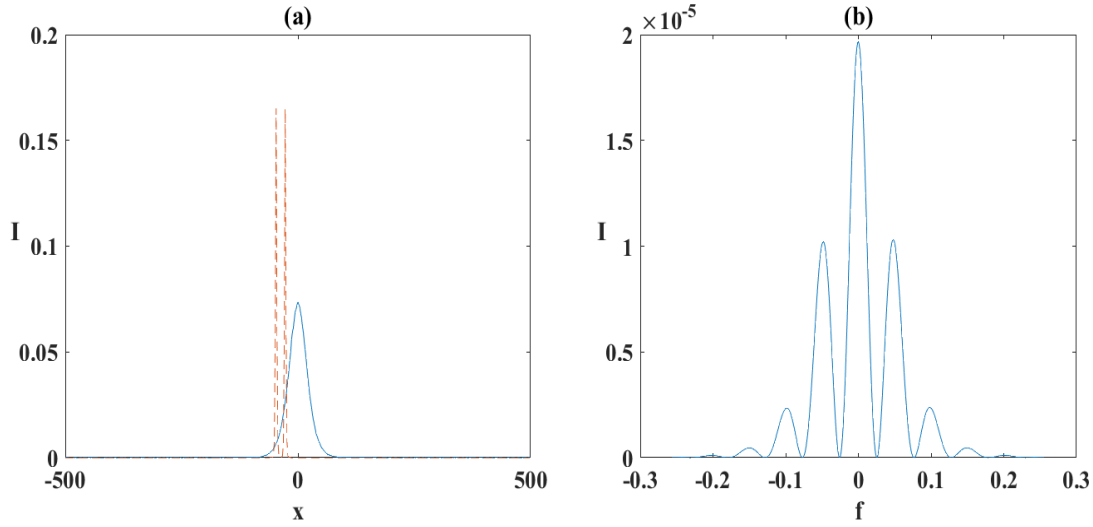

Figure 3.31: Same as fig. 3.28, but for the SNR is 58.5.

In the above cases the OFCs are not very good. We got good OFCs (which are having more teeth that helps in precise measurement) for certain S/N ratio (e.g., 66, 69, 74 76) which are given in fig. 3.32 to 3.35, However at some S/N ratio no OFC is generated. Please see fig. 3.36, that corresponds to S/N=72.5.

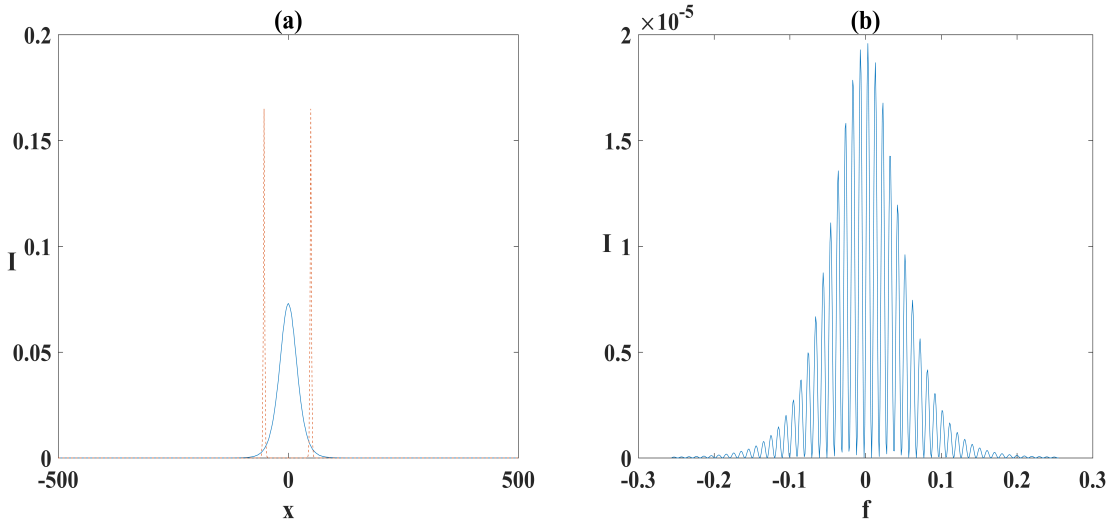

Figure 3.32: (a) The generation of a pair of cavity solitons(tall thin dotted lines) from an input signal(short blue-white profile) and (b) is the corresponding OFC. Here the SNR is 66.

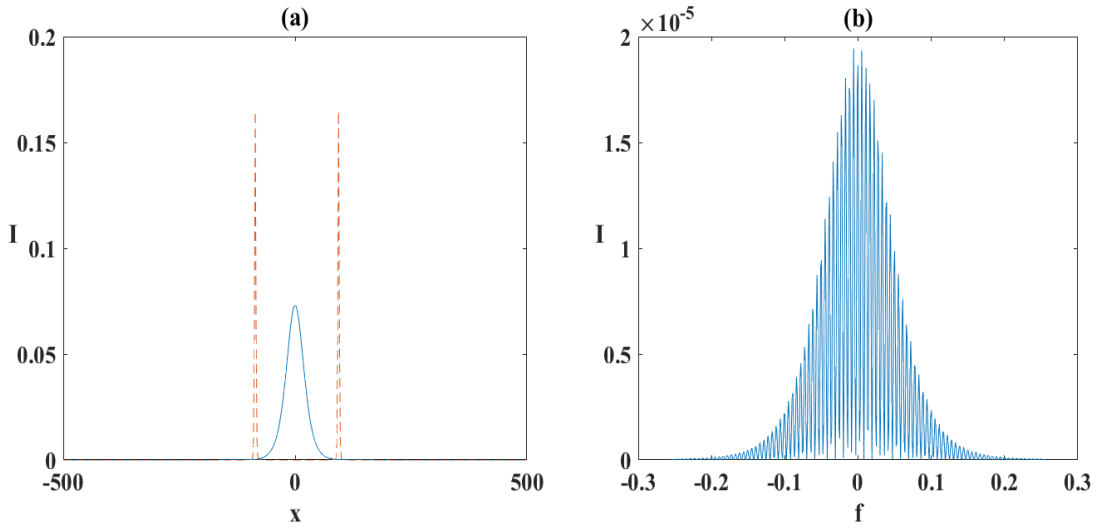

Figure 3.33: (a) The generation of a pair of cavity solitons(tall thin dotted lines) from an input signal(short blue-white profile) and (b) is the corresponding OFC. Here the SNR is 69.

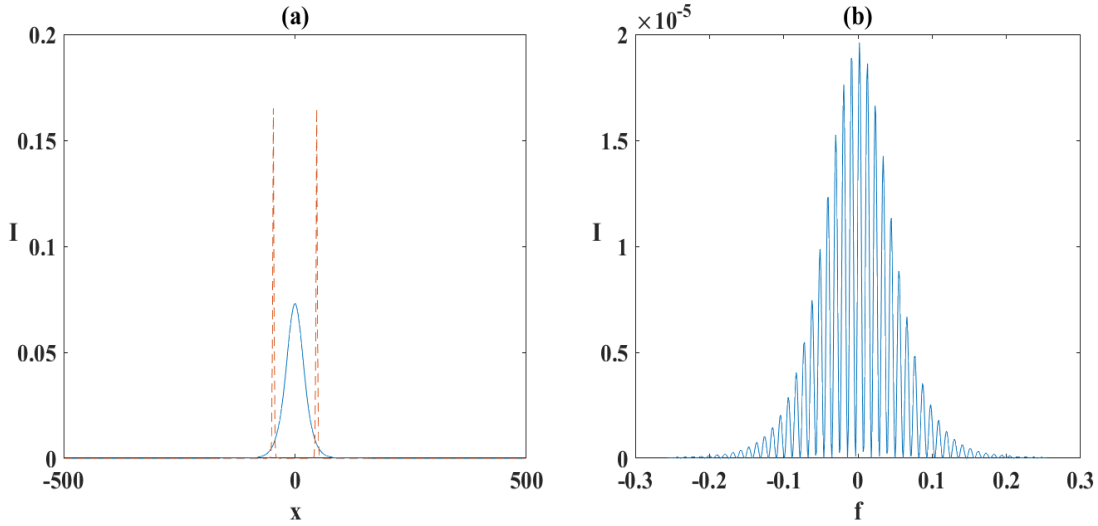

Figure 3.34: (a) The generation of a pair of cavity solitons(tall thin dotted lines) from an input signal(short blue-white profile) and (b) is the corresponding OFC. Here the SNR is 74.

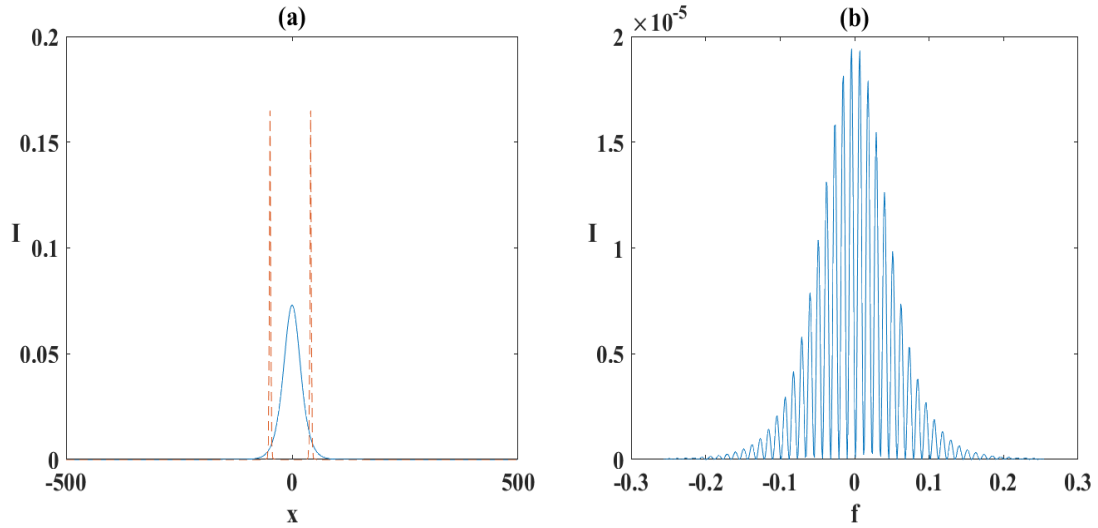

Figure 3.35: (a) The generation of a pair of cavity solitons(tall thin dotted lines) from an input signal(short blue-white profile) and (b) is the corresponding OFC. Here the SNR is 76.

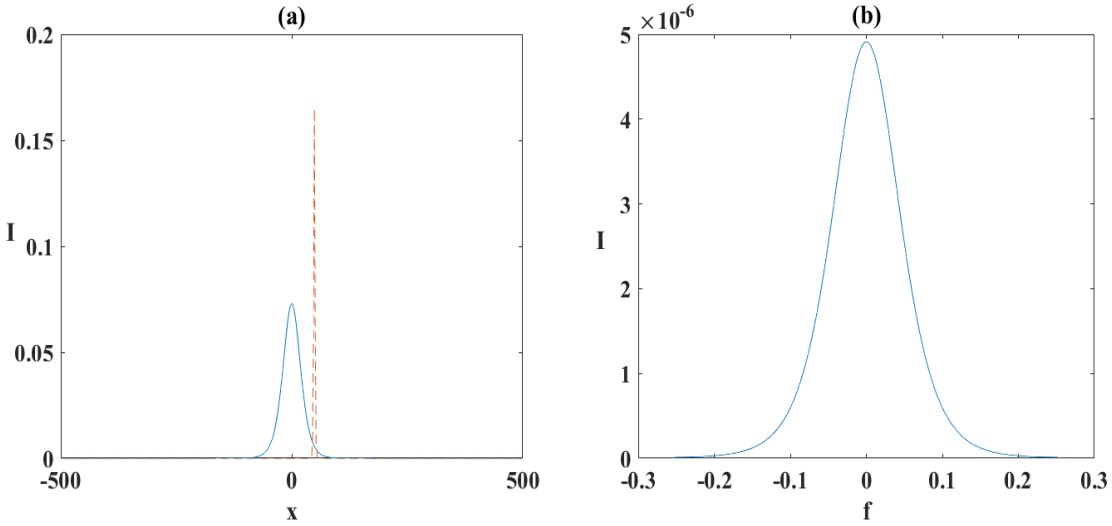

Figure 3.36: (a) The generation of a single cavity soliton(tall thin dotted lines) from an input signal(short blue-white profile) and (b) no OFC is observed. Here the SNR is 72.5.

3.2.2 Optical frequency comb at wavelength 1550nm:

We now find the effect of noise on OFC for operational wavelength 1550nm. This wavelength assures least loss in the optical fibre communication system.

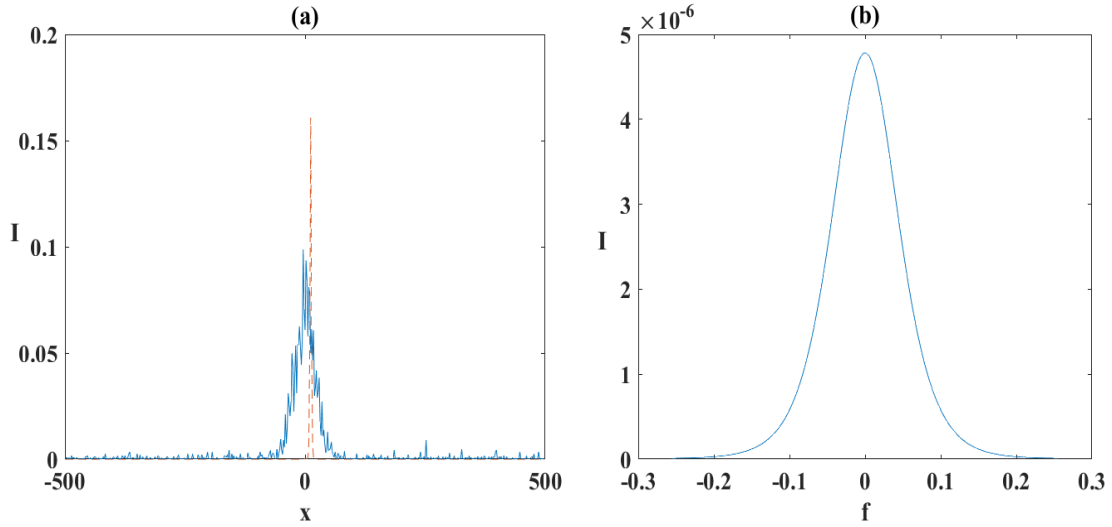

Figure 3.37: (a) The generation of a single cavity soliton(tall thin dotted lines) from an input signal(short blue-white profile) and (b)no OFC is obtained in this case. Here the SNR is 32.

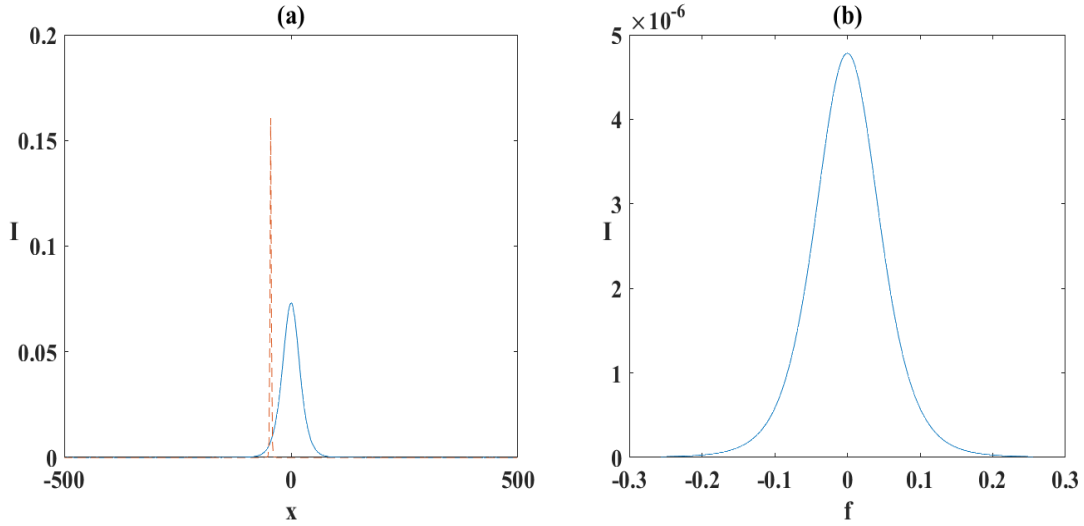

Figure 3.38: (a) The generation of a single cavity soliton(tall thin dotted lines) from an input signal(short blue-white profile) and (b) no OFC is observed. Here the SNR is 66.

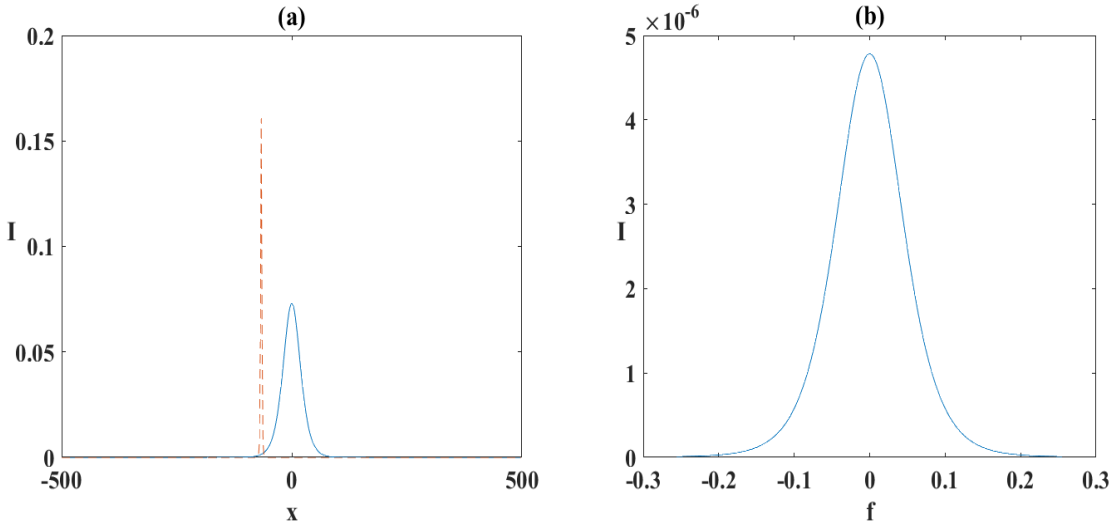

Figure 3.39: (a) The generation of a single cavity soliton(tall thin dotted lines) from an input signal(short blue-white profile) and (b) no OFC. Here the SNR is 72.5.

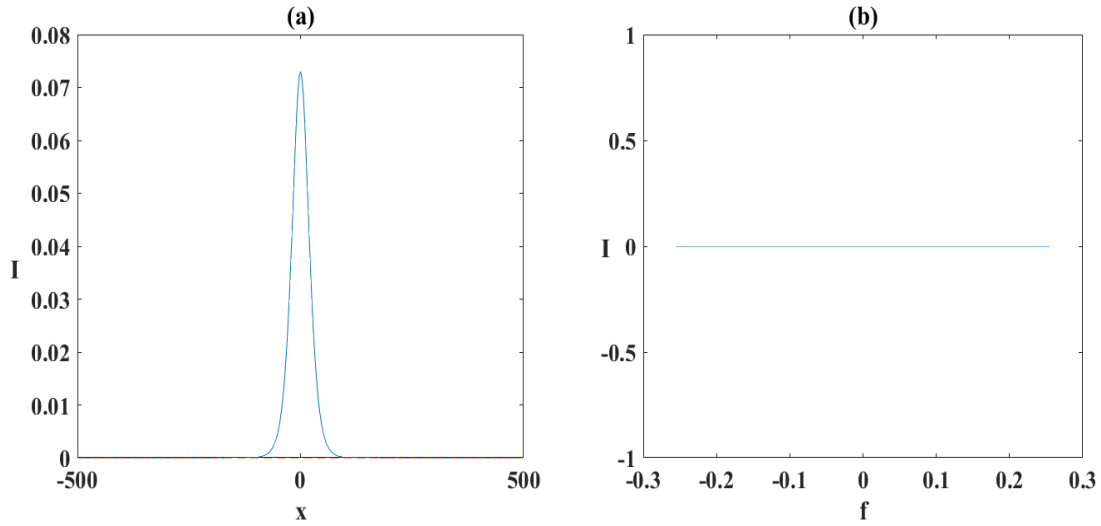

Figure 3.40: (a) the SNR is 74 no cavity soliton is generated from the input signal(short blue-white profile) and (b) so no OFC is generated.

Here, also we get OFC in certain S/N ratios. These are depicted in following figures.

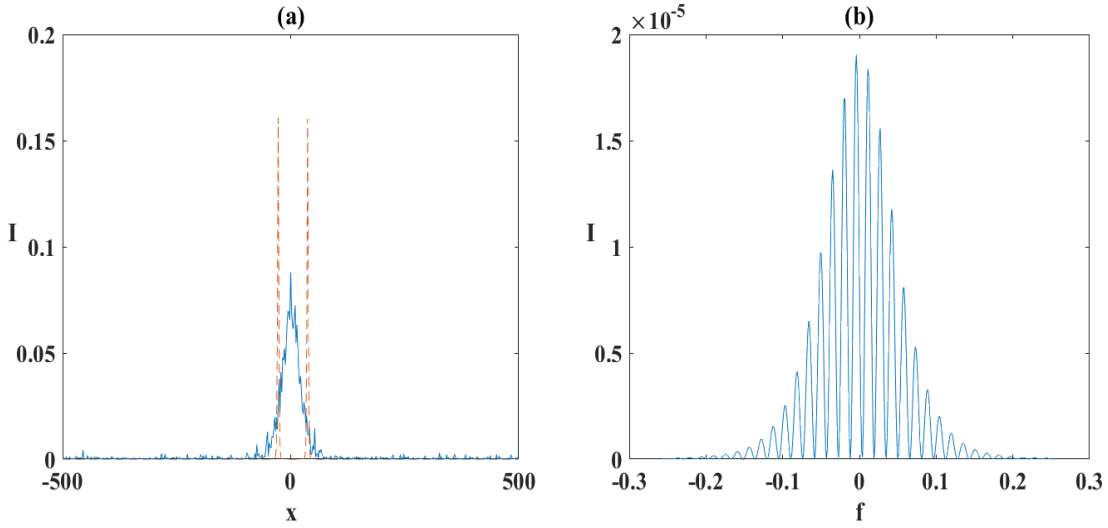

Figure 3.41: (a) The generation of a pair of cavity solitons(tall thin dotted lines) from an input signal(short blue-white profile) and (b) is the corresponding OFC. Here the SNR is 34.

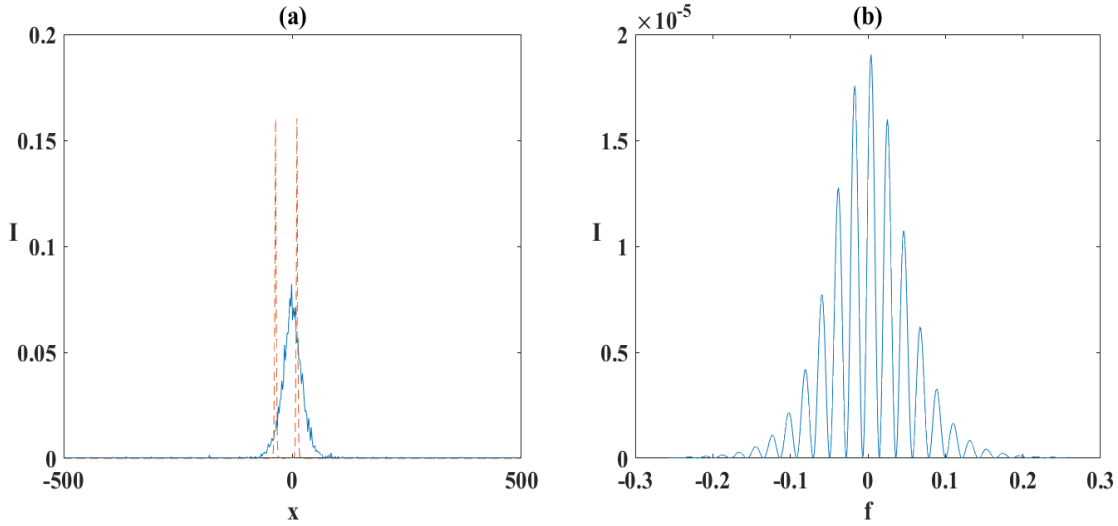

Figure 3.42: Same as fig. 3.38, but for the SNR is 40.

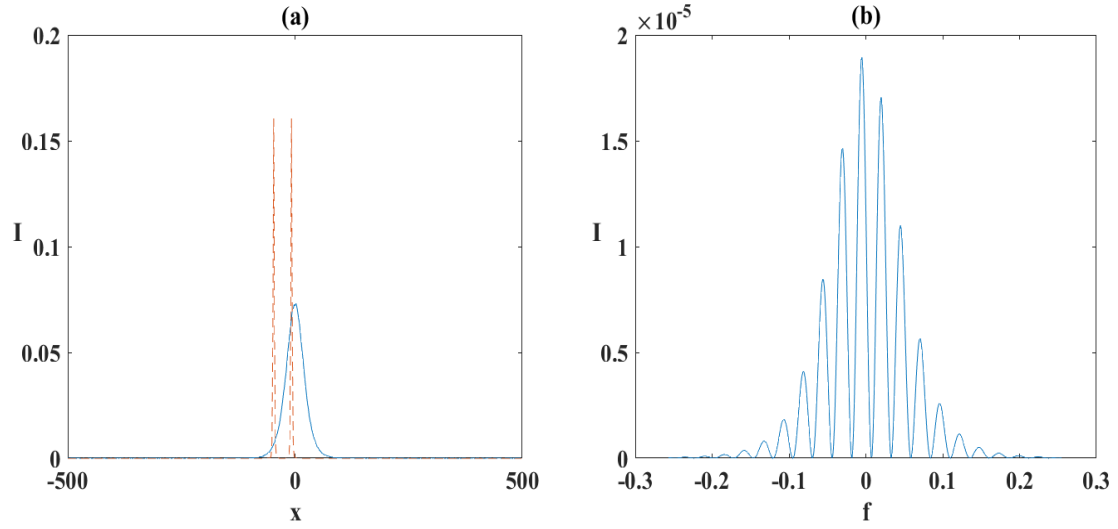

Figure 3.43: Same as fig. 3.38, but for the SNR is 58.5.

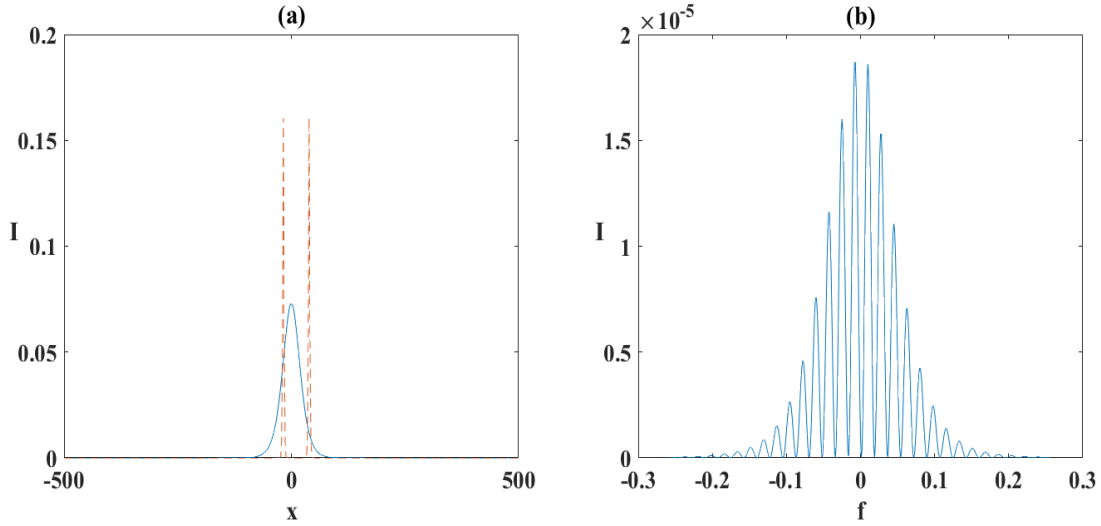

Figure 3.44: Same as fig. 3.38, but for the SNR is 69.

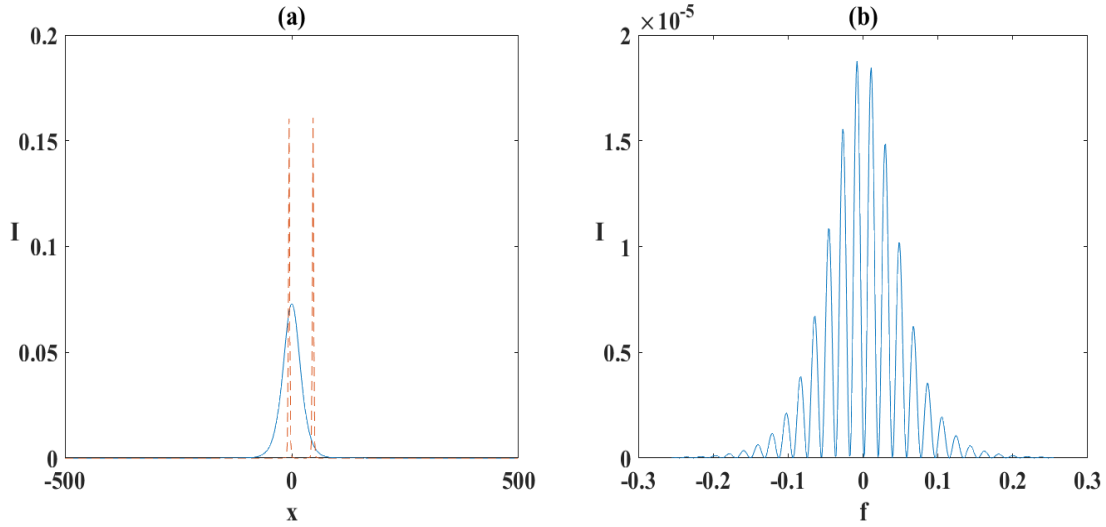

Figure 3.45: Same as fig. 3.38, but for the SNR is 76.

3.2.3 Optical frequency comb at wavelength 2000nm:

We now find the effect of noise for operational wavelength 2000nm.

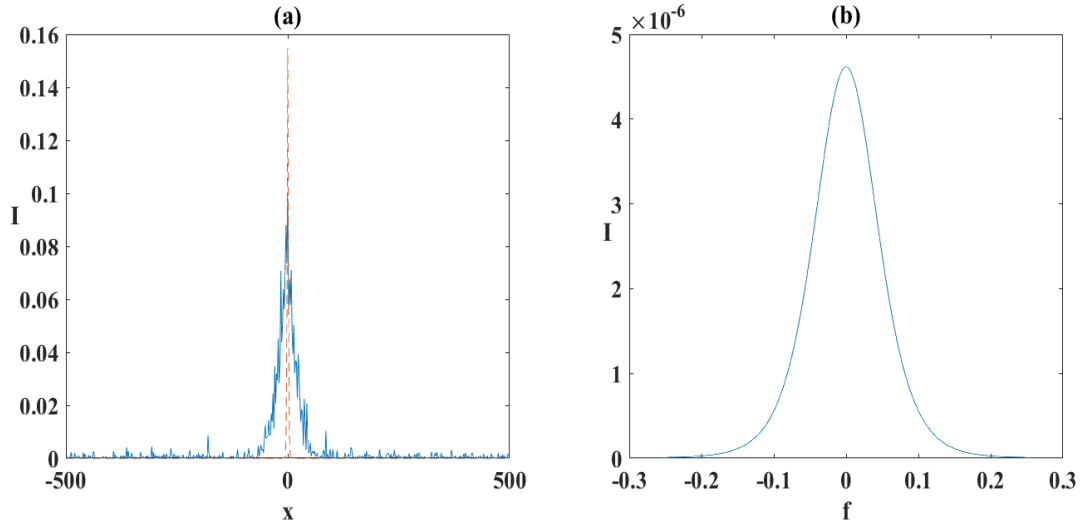

Figure 3.46: (a) The generation of a single cavity soliton(tall thin dotted lines) from an input signal(short blue-white profile) and (b) no OFC is observed. Here the SNR is 32.

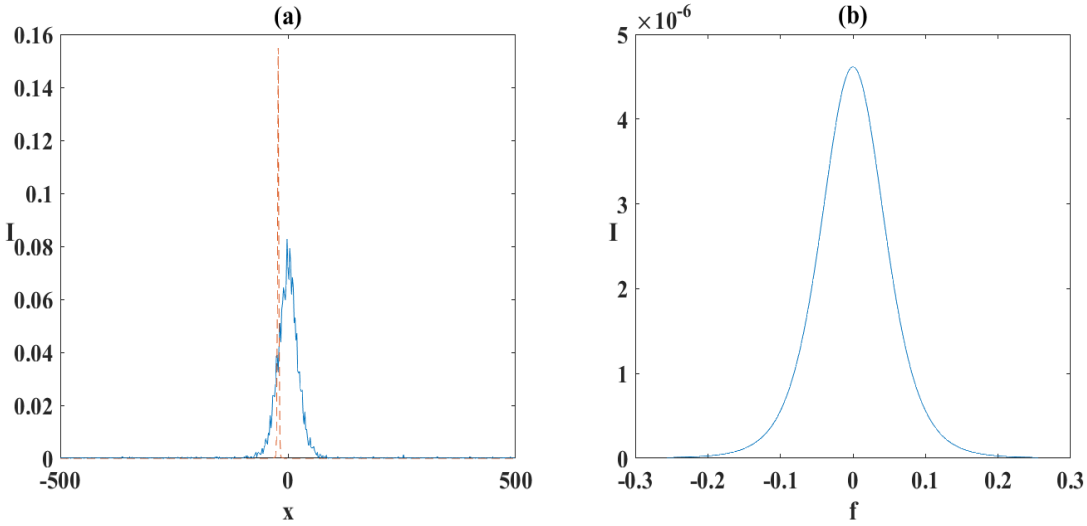

Figure 3.47: Same as fig. 3.46, but for the SNR is 40.

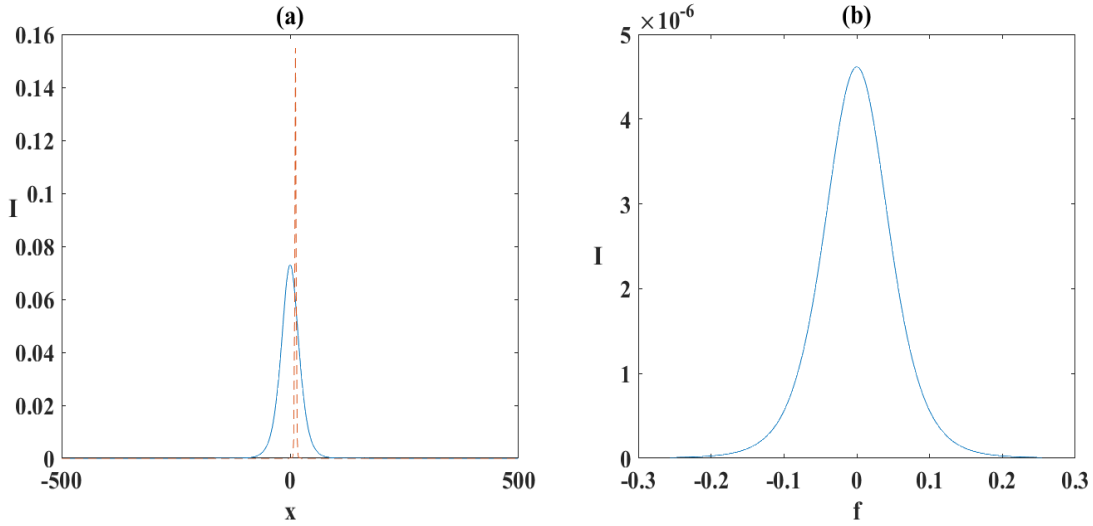

Figure 3.48: Same as fig. 3.46, but for the SNR is 72.5.

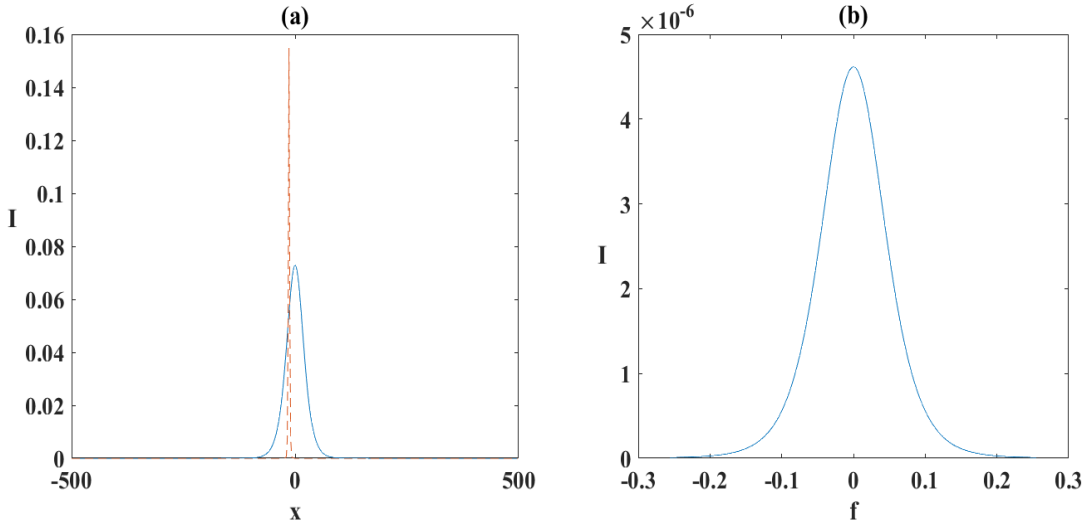

Figure 3.49: Same as fig. 3.46, but for the SNR is 74.

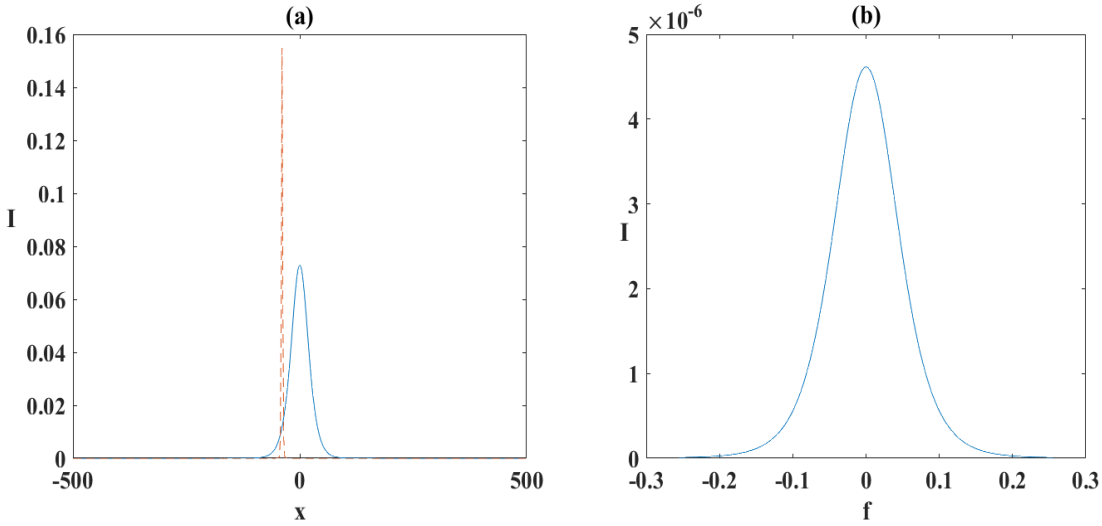

Figure 3.50: Same as fig. 3.46, but for the SNR is 76.

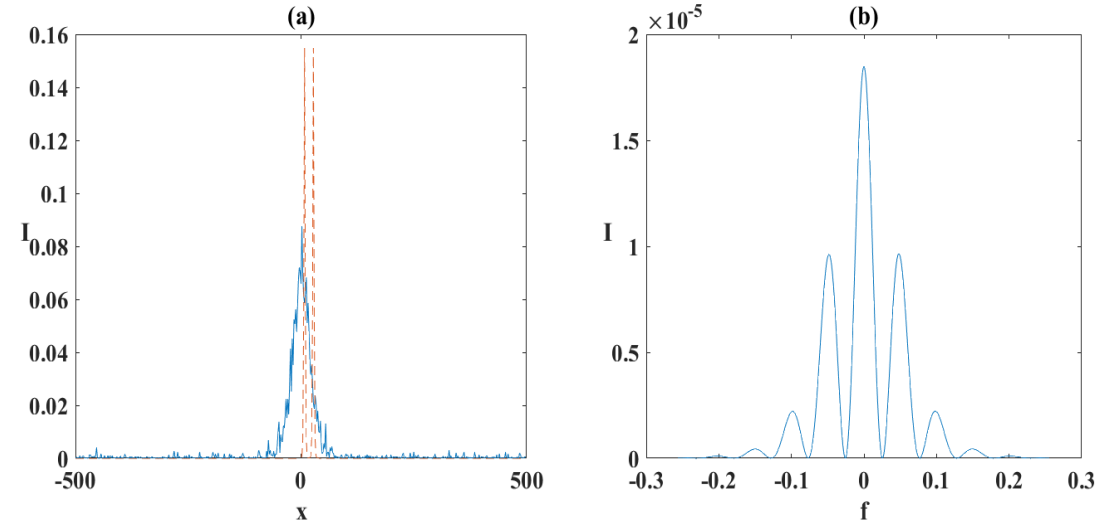

Figure 3.51: (a) The generation of a pair of cavity solitons(tall thin dotted lines) from an input signal(short blue-white profile) and (b) is the corresponding OFC. Here the SNR is 34.

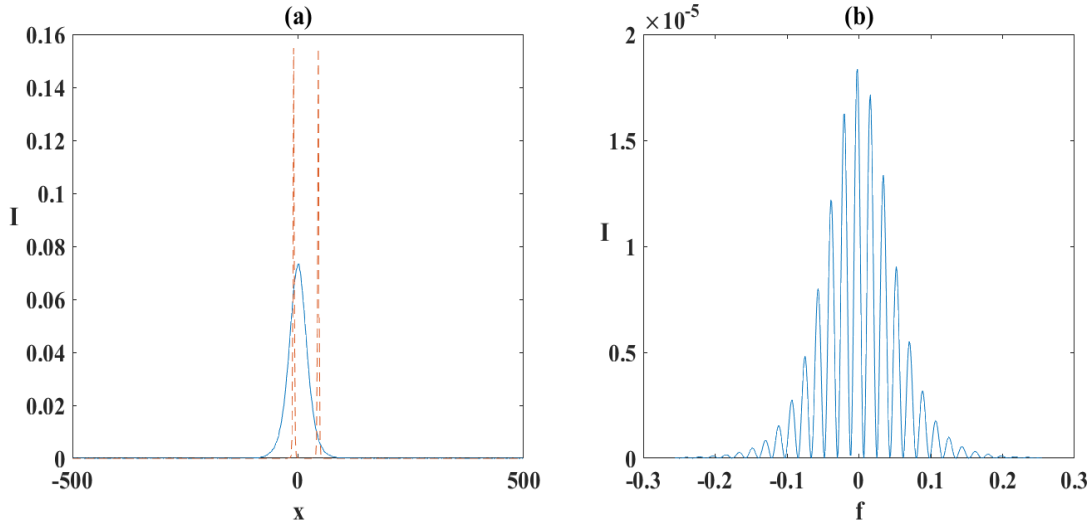

Figure 3.52: Same as fig. 3.51, but for the SNR is 58.5.

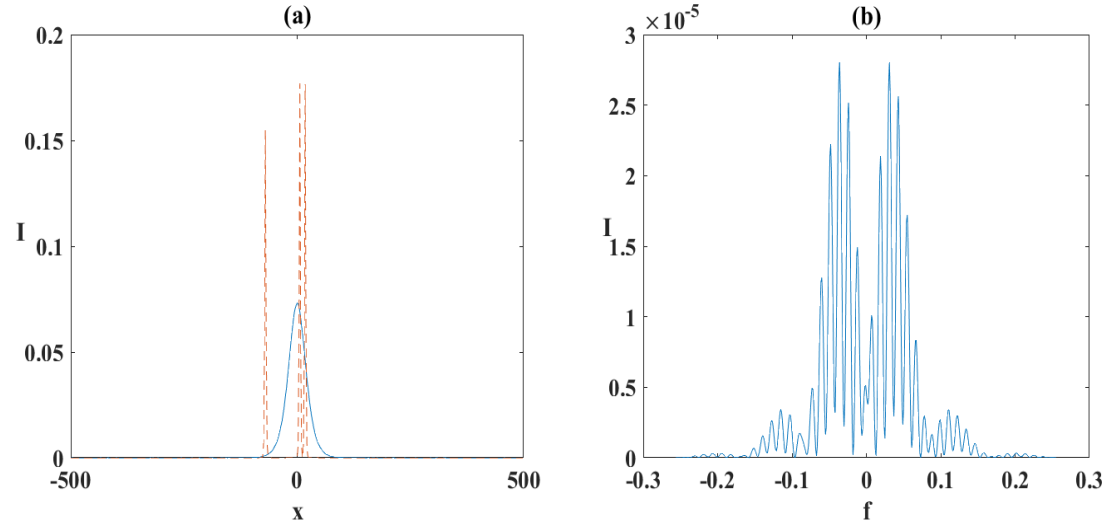

Figure 3.53: (a) The generation of a three cavity solitons(tall thin dotted lines) from an input signal(short blue-white profile) and (b) is the corresponding OFC. Here the SNR is 66.

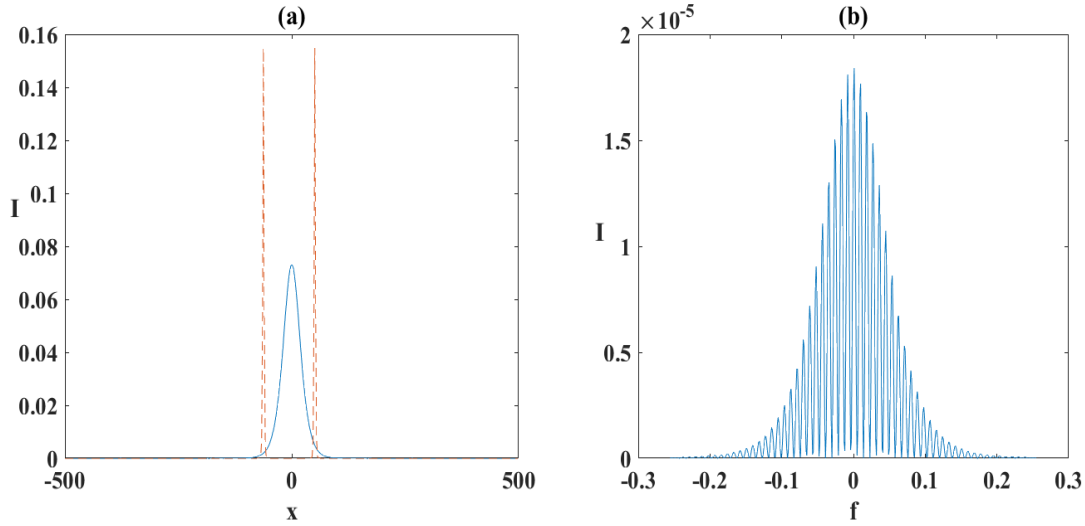

Figure 3.54: Same as fig. 3.51, but for the SNR is 69.

It has been observed that OFC is generated for fewer S/N ratios in 2000nm in comparison to the other wavelengths.

Chapter 4

Conclusion of the Results

4.1 Conclusion

In this work, we study the different sets of OFC for different ranges of S/N ratio. We learned that there is a huge effect of noise on OFC and soliton as well. For different values of the S/N ratio, different types of OFCs are generated. We investigated the S/N ratio from 26.5-49.5 and 32-76. The OFCs generated for the range 26.5-49.5 have broad teeth, i.e., the difference between the teeth of OFC is large. Whereas for the range 32-76, the narrow teeth OFCs are generated. For some values of the S/N ratio, like 20.5, 21, 30, 41.5, 50.5, and 56, poor OFCs are generated. The value of the S/N ratio is greater than 80 (80<S/N>100), and the narrow peaks and the same pattern OFC is generated. After seeing the effect of noise on the OFC, we investigate the effect of wavelengths on OFC. We investigate the OFCs for the different values of wavelength, namely 1330nm, 1550nm, and 2000nm. For the higher values of wavelength, poor OFCs are generated as compared to the lower values of wavelength, where narrow teeth OFCs are generated. We find good OFCs for wavelengths of 1330nm and 1550nm.

4.2 Applications and future scope

The optical frequency comb has a large range of applications in various fields. Our investigation is used to study the experimental verification of the OFC. Different sets of optical frequency comb which are collected from our investigation are used for different levels of research. Our current investigation is further extended to many other works. This investigation is not enough to see the effect of noise and wavelength on optical frequency comb; it is further extended to see the variation in optical frequency comb with the change in noise and wavelength.

Bibliography

[1] https://www.nist.gov/topics/physics/optical-frequency-combs

[2] Fortier, T. and Baumann, E., 2019. 20 years of developments in optical frequency comb technology and applications. Communications Physics, 2(1), pp.1-16.

[3] Ye, J. and Cundiff, S.T. eds., 2005. Femtosecond optical frequency comb: principle, operation and applications. Springer Science & Business Media.

[4] Diddams, S.A., 2010. The evolving optical frequency comb. JOSA B, 27(11), pp.B51-B62

[5] https://en.wikipedia.org/wiki/Frequency_comb

[6] https://en.wikipedia.org/wiki/Frequency_comb

[7] Kippenberg TJ, Holzwarth R, Diddams SA. Microresonator-based optical frequency combs. science. 2011 Apr 29;332(6029):555-9

[8] https://www.youtube.com/watch?v=njtHAxqo7bU

[9] https://www.degruyter.com/document/doi/10.1515/nanoph-2016-0019/html

[10] Cano EP, de Dios Fernandez C, Serrano ÁR, Ortsiefer M, Meissner P, Acedo P.

[11] Experimental study of VCSEL-based optical frequency comb generators. IEEE Photonics Technology Letters. 2014 Aug 27;26(21):2118-21

[12] Anandarajah PM, Maher R, Xu YQ, Latkowski S, O'carroll J, Murdoch SG, Phelan R, O'Gorman J, Barry LP. Generation of coherent multicarrier signals by gain switching of discrete mode lasers. IEEE Photonics Journal. 2011 Jan 13;3(1):112-22.

[13] H. Wahlquist, J. Chem. Phys. 35, 1708 (1961).

[14] P. Kluczynski, J. Gustafsson, A. M. Lindberg, and O. Axner, Spectrochim. Acta B 56, 1277 (2001).

[15] G. C. Bjorklund, Opt. Lett. 5, 15 (1980).

[16] A. O'Keefe and D. A. G. Deacon, Rev. Sci. Instrum. 59, 2544 (1988).

[17] B. A. Paldus and A. A. Kachanov, Can. J. Phys. 83, 975 (2005).

[18] Inaba, H., Daimon, Y., Hong, F.L., Onae, A., Minoshima, K., Schibli, T.R., Matsumoto, H., Hirano, M., Okuno, T., Onishi, M. and Nakazawa, M., 2006. Long-term measurement of optical frequencies using a simple, robust and low-noise fiber based frequency comb. Optics Express, 14(12), pp.5223-5231.

[19] G. J. Dick, Proceedings of the Precise Time and Time Interval Meeting, 1988 (unpublished)

[20] G. Santarelli, C. Audoin, A. Makdissi, P. Laurent, G. J. Dick, and A. Clairon, IEEE Trans. Ultrason. Ferroelectr. Freq. Control https://doi.org/10.1109/58.710548 45, 887 (1998).

[21] Millo, J., Abgrall, M., Lours, M., English, E.M.L., Jiang, H., Guéna, J., Clairon, A., Tobar, M.E., Bize, S., Le Coq, Y. and Santarelli, G., 2009. Ultralow noise microwave generation with fiber-based optical frequency comb and application to atomic fountain clock. Applied Physics Letters, 94(14), p.141105.

[22] G. Santarelli, P. Laurent, P. Lemonde, A. Clairon, A. G. Mann, S. Chang, A. N. Luiten, and C. Salomon, Phys. Rev. Lett.

[23] J. D. Prestage, S. K. Chung, L. Lim, and T. Le, Proceedings of the SPIE 667306, 2007 (unpublished).

[24] S. S. Doeleman, Proceedings of the Seventh Symposium on Frequency Standard Metrology, 2008 (unpublished).

[25] Diddams SA. The evolving optical frequency comb. JOSA B. 2010 Nov 1;27(11):B51-62.

[26] Savchenkov AA, Matsko AB, Ilchenko VS, Solomatine I, Seidel D, Maleki L. Tunable optical frequency comb with a crystalline whispering gallery mode resonator. Physical review letters. 2008 Aug 25;101(9):093902.

[27] Hansson T, Wabnitz S. Frequency comb generation beyond the Lugiato–Lefever equation: multi-stability and super cavity solitons. JOSA B. 2015 Jul 1;32(7):1259-66.

[28] A. Hasegawa and F. Tappert, Appl. Phys. Lett. 23, 142 (1973).

[29] G. Agrawal, Nonlinear Fiber Optics, (2007) Academic Press, San Diego.

[30] J. S. Russell, Report on waves, volume Report of the 14th meeting, pp. 311–390, London, September 1844, Brit. Assoc. Adv. Sci.

[31] Xu, M., He, M., Zhu, Y., Yu, S. and Cai, X., 2022. Flat optical frequency comb generator based on integrated lithium niobate modulators. Journal of Lightwave Technology, 40(2), pp.339-345.

[32] W.J. Firth, G.K. Harkness, Cavity Solitons, Asian J. Phys. 7 (1998) 665–677

[33] F. Arecchi, S. Boccaletti, and P. Ramazza, Phys. Rep. 318, 1-83 (1999).

[34] Wang, T., Wu, J.L., Yang, K., Yang, Y.D., Xiao, J.L. and Huang, Y.Z., 2022. Flat Self-Oscillating Parametric Optical Frequency Comb Based on a Dual-Mode Microcavity Laser. IEEE Photonics Technology Letters, 34(6), pp.325-328.

[35] T. Ackemann, W. J. Firth, and G.-L. Oppo, Fundamentals and applications of spatial dissipative solitons in photonic devices, in Advances in Atomic Molecular and Optical Physics, edited by E. Arimondo, P. R. Berman, and C. C. Lin, volume 57, chap. 6, pp. 323–421, Academic Press, 2009.

[36] J. Murray, Mathematical Biology II (Springer-Verlag New York, 2003).

[37] J. Ross, S. C. M¨uller, and C. Vidal, 240, 460-465 (1988).

[38] N. B. Abraham and W. J. Firth, J. Opt. Soc. Am. B 7, 951-962 (1990).

[39] Michalzik R, editor. VCSELs: fundamentals, technology and applications of vertical-cavity surface-emitting lasers. Springer; 2012 Oct 16.

[40] Iga K. Vertical-cavity surface-emitting laser: its conception and evolution. Japanese Journal of Applied Physics. 2008 Jan 18;47(1R)

[41] Hargrove LE, Fork RL, Pollack MA. Locking of He–Ne laser modes induced by synchronous intracavity modulation. Applied Physics Letters. 1964 Jul 1;5(1):4-5.

[42] https://tudr.thapar.edu:8443/jspui/handle/10266/6005.

[43] Scroggie, A.J., Firth, W.J. and Oppo, G.L., 2009. Cavity-soliton laser with frequency-selective feedback. Physical Review A, 80(1), p.013829.

[44] https://www.rp-photonics.com/vertical cavity surface emitting lasers.

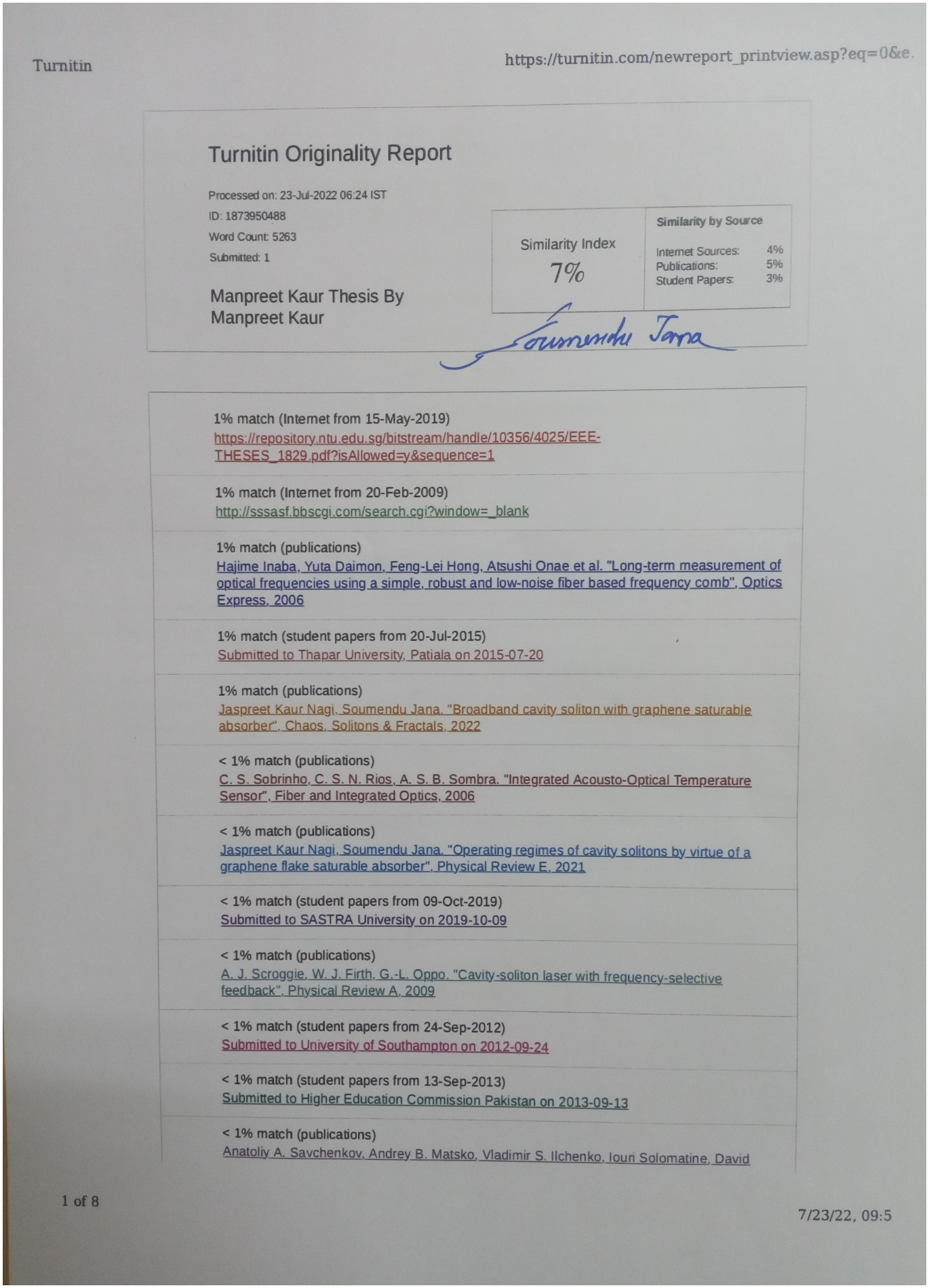

Turnitin https://turnitin.com/newreport_printview.asp?eq=0&e.

Turnitin Originality Report

Processed on: 23-Jul-2022 06:24 IST
ID: 1873950488
Word Count: 5263
Submitted: 1

Manpreet Kaur Thesis By Manpreet Kaur

Similarity Index	Similarity by Source	
7%	Internet Sources:	4%
	Publications:	5%
	Student Papers:	3%

Soumendu Jana

1% match (Internet from 15-May-2019)
https://repository.ntu.edu.sg/bitstream/handle/10356/4025/EEE-THESES_1829.pdf?isAllowed=y&sequence=1

1% match (Internet from 20-Feb-2009)
http://sssasf.bbscgi.com/search.cgi?window=_blank

1% match (publications)
Hajime Inaba, Yuta Daimon, Feng-Lei Hong, Atsushi Onae et al. "Long-term measurement of optical frequencies using a simple, robust and low-noise fiber based frequency comb", Optics Express, 2006

1% match (student papers from 20-Jul-2015)
Submitted to Thapar University, Patiala on 2015-07-20

1% match (publications)
Jaspreet Kaur Nagi, Soumendu Jana. "Broadband cavity soliton with graphene saturable absorber", Chaos, Solitons & Fractals, 2022

< 1% match (publications)
C. S. Sobrinho, C. S. N. Rios, A. S. B. Sombra. "Integrated Acousto-Optical Temperature Sensor", Fiber and Integrated Optics, 2006

< 1% match (publications)
Jaspreet Kaur Nagi, Soumendu Jana. "Operating regimes of cavity solitons by virtue of a graphene flake saturable absorber", Physical Review E, 2021

< 1% match (student papers from 09-Oct-2019)
Submitted to SASTRA University on 2019-10-09

< 1% match (publications)
A. J. Scroggie, W. J. Firth, G.-L. Oppo. "Cavity-soliton laser with frequency-selective feedback", Physical Review A, 2009

< 1% match (student papers from 24-Sep-2012)
Submitted to University of Southampton on 2012-09-24

< 1% match (student papers from 13-Sep-2013)
Submitted to Higher Education Commission Pakistan on 2013-09-13

< 1% match (publications)
Anatoliy A. Savchenkov, Andrey B. Matsko, Vladimir S. Ilchenko, Iouri Solomatine, David

1 of 8 7/23/22, 09:5